Surprising Formation of Highly Substituted Azulenes on Thermolysis of 4,5,6,7,8-Pentamethyl-2*H*-cyclohepta[*b*]furan-2-one and Heptalene Formation with the New Azulenes

by **Vit Lellek** and **Hans-Jürgen Hansen***

Organisch-chemisches Institut der Universität Zürich, Winterthurerstr. 190, CH-8057 Zürich

Dedicated to *Edgar Heilbronner* on the occasion of his 80th birthday

Der Mensch kommt nicht um die Tatsache herum, dass die Sinne zwar als höchste Herren seine Erkenntnisfähigkeit bestimmen, ihm aber keine Sicherheit bieten, da sie in jeder Lage sich leicht täuschen lassen.

Michel de Montaigne, Essais (Übers. Hans Stilett)

Heating of 4,5,6,7,8-pentamethyl-2*H*-cyclohepta[*b*]furan-2-one (**1a**) in decalin at temperatures $>170°$ leads to the development of a blue color, typical for azulenes. It belongs, indeed, to two formed azulenes, namely 4,5,6,7,8-pentamethyl-2-(2,3,4,5,6-pentamethylphenyl)azulene (**4a**) and 4,5,6,7,8-pentamethylazulene (**5a**) (*cf. Scheme 2* and *Table 1*). As a third product, 4,5,6,7-tetramethyl-2-(2,3,4,5,6-pentamethylphenyl)-1*H*-indene (**6a**) is also found in the reaction mixture. Neither 4,6,8-trimethyl-2*H*-cyclohepta[*b*]furan-2-one (**1b**) nor 2*H*-cyclohepta[*b*]furan-2-one (**1c**) exhibit, on heating, such reactivity. However, heating of mixtures **1a**/**1b** or **1a**/**1c** results in the formation of crossed azulenes, namely 4,6,8-trimethyl-2-(2,3,4,5,6-pentamethylphenyl)azulene (**4ba**) and 2-(2,3,4,5,6-pentamethylphenyl)azulene (**4ca**), respectively (*cf. Scheme 3*). The formation of small amounts of 4,6,8-trimethylazulene (**5ba**) and azulene (**5ca**), respectively, besides 1*H*-indene **6a** is also observed. The observed product types speak for an $[8+2]$-cycloaddition reaction between two molecules of **1a** or between **1b** and **1c**, respectively, with **1a**, whereby **1a** plays in the latter two cases the part of the two-atom component (*cf. Figs. 5–7* and *Schemes 4–6*). Strain release, due to the five adjacent Me groups in **1a**, in the $[8+2]$-cycloaddition step seems to be the driving force for these transformations (*cf. Table 3*), which are further promoted by the consecutive loss of two molecules of CO_2 and concomitant formation of the 10π-electron system of the azulenes. The new azulenes react with dimethyl acetylenedicarboxylate (ADM) to form the corresponding dimethyl heptalene-4,5-dicarboxylates **20**, **22**, and **24** (*cf. Scheme 7*), which give thermally or photochemically the corresponding double-bond-shifted (DBS) isomers **20′**, **22′**, and **24′**, respectively. The five adjacent Me groups in **20**/**20′** and **24**/**24′** exert a certain buttressing effect, whereby their thermal DBS process is distinctly retarded in comparison to **22**/**22′**, which carry 'isolated' Me groups at C(6), C(8), and C(10). This view is supported by X-ray crystal-structure analyses of **22** and **24** (*cf. Fig. 8* and *Table 5*).

1. Introduction. – Recently, we reported on the synthesis of highly alkylated 2*H*-cyclohepta[*b*]furan-2-ones by vacuum flash pyrolysis (VFP) of polyalkylphenyl prop-2-ynoates [1], following a procedure originally described by *Trahanovsky et al.* [2]. We also showed, *inter alia*, that 4,5,6,7,8-pentamethyl-2*H*-cyclohepta[*b*]furan-2-one (**1a**) reacts thermally with 1-(cyclohex-1-en-yl)pyrrolidine in toluene to give the corresponding 1,2,3,4-tetrahydrobenz[*a*]azulene **2** (*Scheme 1*) according to a general method of azulene synthesis established by *Nozoe et al.* (see ref. cit. in [1]). Since we were especially interested in the synthesis of 4,5,6,7,8-pentamethyl-(**3a**) as well as 1,4,5,6,7,8-hexamethylazulene (**3b**), we tested a whole number of electron-donor substituted ethenes and propenes in the thermal addition reaction with **1a** – but with only moderate

Scheme 1

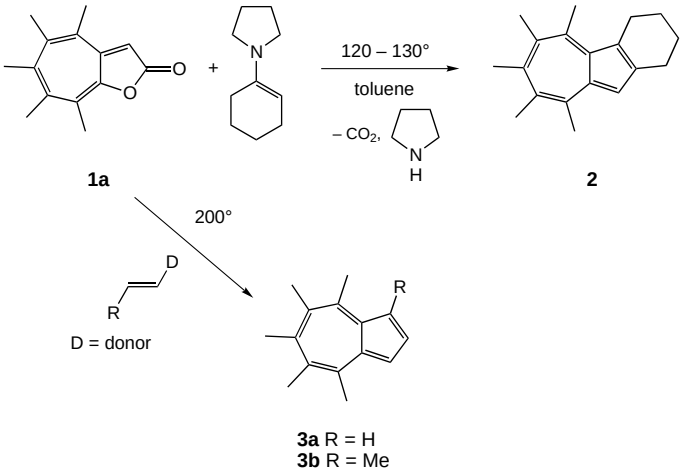

success [3]. In particular, we did not succeed in reacting **1a** thermally with easily available enol ethers as the most convenient source for the necessary two C-atoms of the azulene core that is formed in the [8 + 2]-cycloaddition step, followed by the loss of CO_2 in a cycloreversion reaction and then by elimination of the corresponding alcohol component of the used enol ether. However, we always observed the development of a blue color, typical for the presence of azulenes in reaction mixtures, so that we thought, at first, that the expected reaction between **1a** and the enol ethers had taken place to a certain extent. But, we then found that the blue color also developed when **1a** was heated in decalin in the absence of any enol ether. Isolation of the blue-color-carrying component left no doubt that it indeed represented an azulene with a $M^{+\bullet}$ peak at *m*/*z* 344 and at least six sharp *s* signals in the ^{1}H-NMR spectrum, attributable to Me groups linked to aromatic C-atoms.

In *Sect. 2*, we describe the details of our investigations on the formation of azulenes upon thermolysis of 4,5,6,7,8-pentamethyl-2*H*-cyclohepta[*b*]furan-2-one (**1a**).

2. Azulene Formation. – Heating a 0.1M solution of **1a** in decalin (= decahydronaphthalene) at 190° during 48 h or at 230° during 3.5 h gave the highest yield of the new azulene **4a** (see *Table 1*). However, thorough chromatography (silica gel, hexane) disclosed the presence of a second azulene **5a** as well as of a colorless compound **6a** (*Scheme 2*). The structure of the second azulene could easily be solved on the basis of its UV/VIS (see *Fig. 1*), ^{1}H- and ^{13}C-NMR, and mass spectra. The UV/VIS spectrum of the main azulene **4a** (see *Fig. 2*) was similar to that of **5a**, however, in contrast to **5a**, with a vibrationally nonstructured, broad azulene absorption band centered at 570 nm. The third colorless compound **6a** exhibited a UV spectrum (see *Fig. 3*) with a strong absorption band at 280 nm that indicated the presence of a styrene-type chromophor. All spectral data of **4a** and **6a** were in full agreement with the proposed structures.

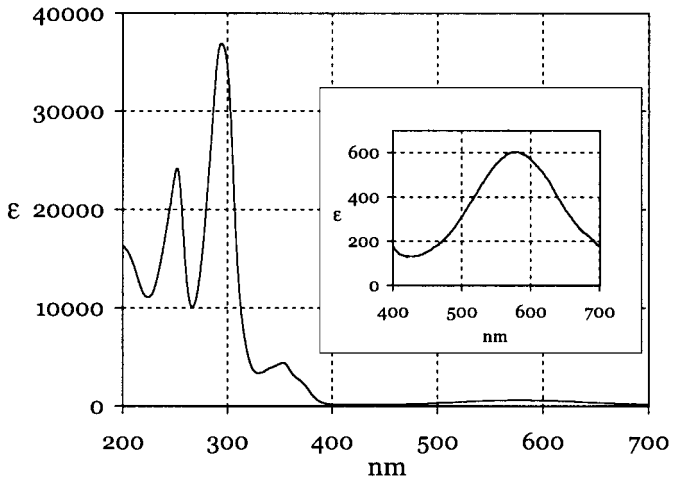

Fig. 1. *UV/VIS Spectrum* (hexane) *of 4,5,6,7,8-pentamethylazulene* (**5a**)

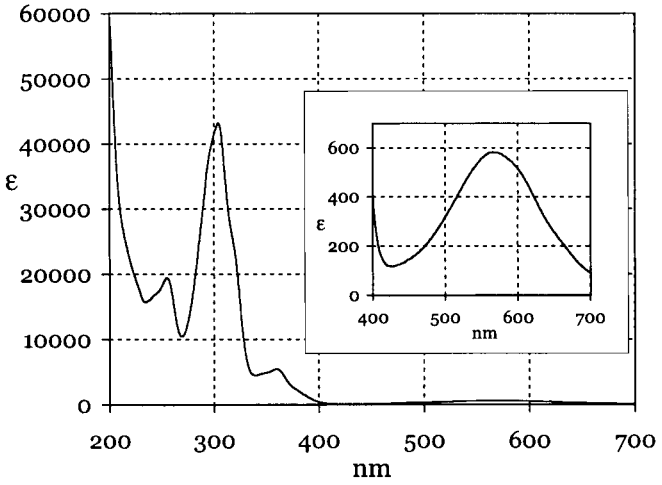

Fig. 2. *UV/VIS Spectrum* (hexane) *of 4,5,6,7,8-pentamethyl-2-(2,3,4,5,6-pentamethylphenyl)azulene* (**4a**)

The ^{1}H-NMR spectrum (C_6D_6) of **5a** exhibited two signals in a ratio of 1:2 in the aromatic region, namely a *t* at 7.81 and a *d* at 7.28 ppm with $J = 4.0$ Hz, characteristic for the nonsubstituted five-membered ring of an azulene. In agreement with this assignment, three sharp *s* signals in a ratio of 2:1:2 at 2.62, 2.11, and 2.09 ppm, attributable to Me–C(4)/Me–C(8), Me–C(6), and Me–C(5)/Me–C(7), respectively, were found in the Me-group region of the spectrum. The MS (70 eV) was in accordance with the assigned structure, since the $M^{+\cdot}$ peak was observed at *m*/*z* 198 (98%) and accompanied by a strong $[M - Me]^+$ peak at *m*/*z* 183 (100%).

The ^{1}H-NMR spectrum (C_6D_6) of **4a** resembled that of **5a**, however, with the exception of there being only one sharp *s* in the aromatic region at 7.30 ppm, counting for two H-atoms, which thus had to be linked symmetrically to the five-membered ring of a 4,5,6,7,8-pentamethylated azulene core. This view was fully supported by the observed *s* signals in the region of aromatically bound Me groups. The already mentioned 6 *s* appeared in a ratio of 2:2:1:2:1:2 at 2.61, 2.27, 2.25, 2.23, 2.17, and 2.14 ppm, respectively. This means that the outer *s* signals at 2.61, 2.17, and 2.14 ppm could be attributed to 5 Me groups at the seven-membered ring of an

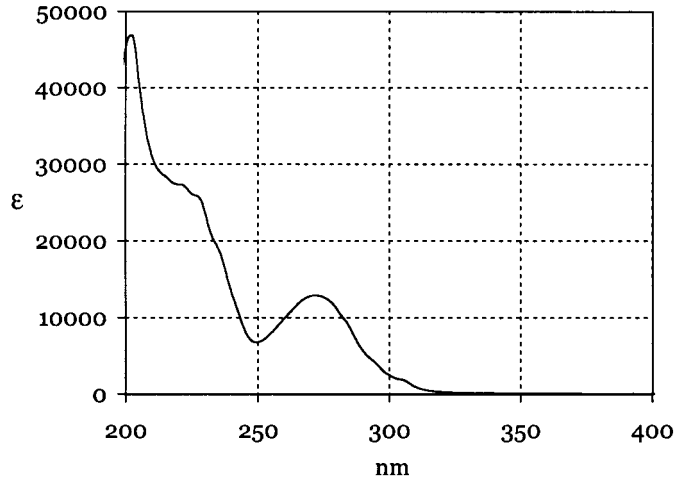

Fig. 3. *UV/VIS Spectrum* (hexane) *of 4,5,6,7-tetramethyl-2-(2,3,4,5,6-pentamethylphenyl)-1*H-*indene* (**6a**)

Table 1. *Product Composition of the Thermal Transformation of 4,5,6,7,8-Pentamethyl-2*H-*cyclohepta[*b*]furan-2-one* (**1a**)

Solvent	Conc. [mol/l]	Time [h]	Temp. [°]	Yield [%]			
				1a	**4a**[a])	**5a**[a])	**6a**[a])
Decalin	0.60	3.5	230	9	29	11	7
Decalin	0.09	48	190	23	53	13	n.d.[b])
Decalin	0.10	24	170	50	3.4	< 0.5	n.d.
Diethylene glycol diethyl ether	0.15	5	230	34	30	6	n.d.
DMSO	0.15	6	210	0[c])	–	–	–

[a]) Yield of purified compound with respect to reacted **1a**. [b]) n.d. = compound observed by TLC and/or HPLC, but yield not determined. [c]) Complete decomposition of **1a**.

Scheme 2[a])

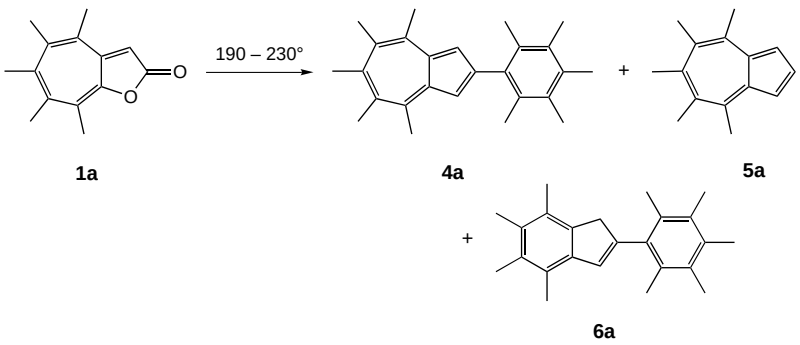

1a **4a** **5a** **6a**

[a]) See *Table 1* for details.

azulene, substituted at C(2) with a residue, which had to account for the other 5, symmetrically arranged Me groups. The only structure that fulfilled these requirements was that of the (pentamethylphenyl)-substituted azulene **4a**. Indeed, the three *s* at 2.27, 2.25, and 2.23 ppm (2 : 1 : 2) could be assigned to Me–C(2′)/Me–C(4′) and Me–C(4′) *via* a ^{1}H-NOESY spectrum of **4a**, and to Me–C(3′)/Me–C(5′), respectively, of the phenyl substituent at C(2). The MS (70 eV) of **4a** with the $M^{+\cdot}$ peak at *m*/*z* 344 (100%), followed by mass peaks at *m*/*z* 329 (49%), 314 (84%), and 299 (55%), indicating the consecutive loss of Me groups, was in full agreement with the structure of **4a**.

The ^{1}H-NMR spectrum (500 MHz, $CDCl_3$) of **6a** displayed in the region for olefinic H-atoms an *s* at 6.72 ppm, counting for one H-atom, and a second *s* at 3.45 ppm, standing for two H-atoms, which could be assigned to a CH_2 group in allylic and/or benzylic surrounding. The region for aromatically positioned Me groups showed three sharp *s* in a ratio of 1 : 2 : 2 at 2.40, 2.26, and 2.14 ppm as well as a broad *s* at 2.30 ppm with a slightly resolved shoulder at the lower-field flank of the signal, counting in a total for 4 Me groups. The presence of indeed 9, aromatically bound Me groups could much better be seen in the ^{13}C-NMR spectrum ($CDCl_3$) of **6a**, which displayed, in the range of 18.2–15.9 ppm, 7 Me signals in a ratio of 2 : 1 : 1 : 2 : 1 : 1 : 1. The fact that the ^{13}C-NMR spectrum indicated two sets of (in pairs equivalent) Me groups was only compatible with the existence of a (pentamethylphenyl) substituent. Indeed, specific ^{1}H-NOE experiments and a ^{1}H-NOESY plot of **6a** admitted the assignment of the two sharp *s* signals at 2.26 and 2.14 ppm to Me–C(3′)/Me–C(5′) and Me–C(2′)/Me–C(6′) of the (pentamethylphenyl) unit. The signal of Me–C(4′) was buried in the broad *s* at 2.30 ppm. The residual signals in the NMR spectra were compatible only with the presence of a 2-substituted 4,5,6,7-tetramethyl-1*H*-indene unit. Moreover, the ^{1}H-NOE experiments demonstrated that the *s* at 2.40 ppm belonged to Me–C(4), whereas Me–C(7) was responsible for the shoulder of the *s* at 2.30 ppm. The two other Me groups at C(5) and C(6), and Me–C(4′) caused the broad *s* at 2.30 ppm. These assignments were confirmed by the fully analyzed ^{13}C-NMR spectrum of **6a**. The mass spectrum (Cl) of **6a** exhibited the expected $[M+1]^+$ peak at *m*/*z* 319 (100%), followed by a weak $[(M+1)-\mathrm{Me}]^{+\cdot}$ peak at *m*/*z* 305 (6%).

The formation of **4a**, **5a**, and **6a** was also observed in diethylene glycol diethyl ether as solvent (*cf. Table 1*). However, in dimethyl sulfoxide (DMSO), complete decomposition of **1a** without product formation was recognized. On the other side, the observed reaction seems to be restricted to **1a**, since neither 4,6,8-trimethyl- (**1b**) nor 4,5,6,7,8-pentafluoro-2*H*-cyclohepta[*b*]furan-2-one (**1d**) gave, on heating in decalin as the most suitable solvent (*cf. Table 1*), any products comparable to those from **1a** (*Scheme 3*). Cross experiments were more successful. When **1a** was heated in 0.1M solution in decalin in the presence of 3 mol-equiv. of **1b**[1]) or equimolar amounts of 2*H*-cyclohepta[*b*]furan-2-one (**1c**) itself, we found the cross products **4ba**/**5ba** and **4ca**/**5ca**, respectively, as well as **6a**, derived from **1a**, in the corresponding reaction mixtures (*Scheme 3*).

We can only speculate on the mechanisms of product formation. Nevertheless, some facts are obvious. The appearance of **4a**, **5a**, and **6a** on thermolysis of **1a** must be the result of bimolecular reactivities of **1a**. The formation of **4a** seems in this context most transparent according to the mass equation: $2 \times [\mathbf{1a} - CO_2] \rightarrow \mathbf{4a}$. The fundamental questions are, therefore: At which state does CO_2 extrusion occur, and what differentiates **1a** from the other 2*H*-cyclohepta[*b*]furan-2-ones? X-Ray crystal-structure analyses of **1a** and, on grounds of comparison, nonsubstituted 2*H*-cyclohepta[*b*]furan-2-one (**1c**) (both this work) as well as AM1 calculations of the structure of 2*H*-cyclohepta[*b*]furan-2-ones, including **1b** and **1d** (see *Table 2*), demonstrate that all of these compounds are perfectly planar, with the only exception of **1a**. It is forced, due to the crowding effect of the Me substituents, in a flat boat-like conformation of the seven-membered ring, comparable to that of heptafulvenes, whereby the calculated

---

[1]) In the presence of equimolar amounts of **1b**, mainly the products of **1a** were formed.

Scheme 3

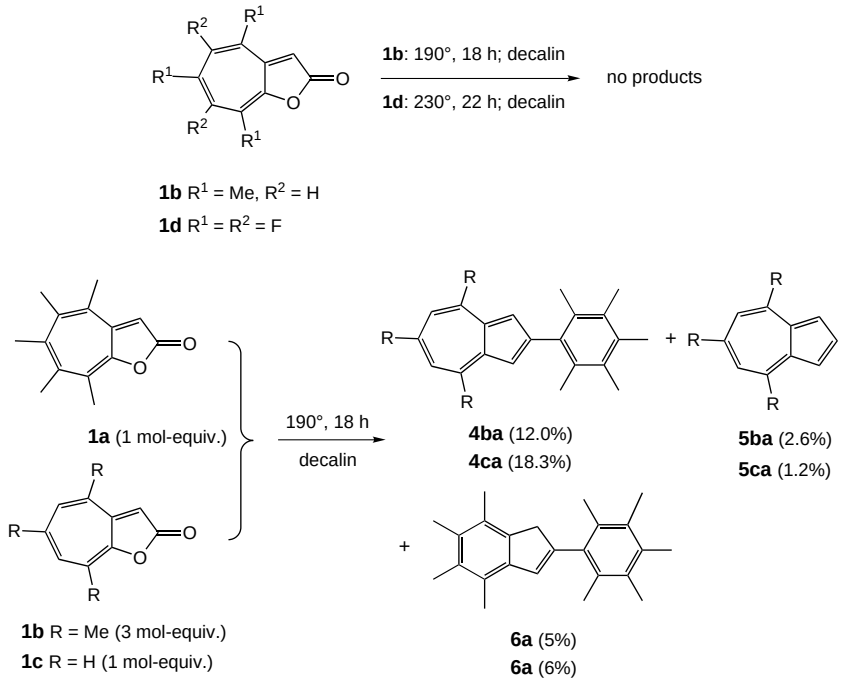

Table 2. *Comparison of Some Structural Data of* 2H-*Cyclohepta[*b*]furan-2-ones* **1** *from an X-Ray Crystal Structure and AM1 Calculations* [a])

Parameter	**1a**[b])	**1b**[b])	**1c**[b])	**1d**[b])
Interatomic distances *d* [pm]:				
C(3)–C(3a)	137.5(3)/137.3	–/137.4	136.1(4)/137.2	–/137.0
C(4)–C(5)	137.6(3)/136.3	–/135.6	134.4(4)/135.1	–/137.9
C(6)–C(7)	138.7(3)/136.5	–/135.8	134.9(4)/135.3	–/137.9
C(8)–C(8a)	136.1(3)/135.7	–/135.7	134.9(4)/135.1	–/136.2
Bond angles ϑ [°]:				
O(1)–C(2)–C(3)	106.9(2)/108.0	–/108.0	106.7(2)/108.0	–/107.8
C(2)–C(3)–C(3a)	109.0(2)/108.0	–/108.0	109.4(2)/108.0	–/107.9
C(5)–C(6)–C(7)	129.6(2)/127.8	–/128.6	129.2(3)/129.8	–/129.8
Torsion angles Θ [°]:				
C(3)–C(3a)–C(4)–C(5)	178.6(2)/168.5	–/180.0	177.8(3)/180.0	–/180.0
C(3)–C(3a)–C(4)–R	0.3(3)/14.8	–/0.0	–/0.0	–/0.0
C(3)–C(3a)–C(8a)–C(8)	179.1(2)/172.2	–/180.0	178.3(4)/180.0	–/180.0
C(3a)–C(4)–C(5)–C(6)	7.4(4)/10.7	–/0.0	0.6(6)/0.0	–/0.0
C(4)–C(5)–C(6)–C(7)	16.3(4)/37.7	–/0.0	0.8(6)/0.0	–/0.0
C(5)–C(6)–C(7)–C(8)	10.9/16.9	–/0.0	1.3(7)/0.0	–/0.0
Least-squares deviations from plane [pm]:				
5-membered ring	0.1/2.9	planar	planar/planar	planar
5- and 7-membered ring	3.1/18.1	planar	planar/planar	planar

[a]) See *Schemes 2* and *3* for substitution patterns. [b]) First value, X-ray data; second value, AM1 data; for an older X-ray crystal-structure analysis of **1c**, see [5].

structure of **1a** is somewhat more twisted than indicated by its X-ray crystal structure. If one compares the calculated ΔH_f° value for **1a** (-22.16 kcal·mol^{-1}) with ΔH_f° (**1a**) = -34.69 kcal·mol^{-1} that is obtained from ΔH_f° (**1c**) = -0.56 kcal·mol^{-1} and the calculated Me-group increments of the corresponding 5 monomethyl-substituted 2*H*-cyclohepta[*b*]furan-2-ones ($\Sigma = -34.13$ kcal·mol^{-1}), the observed difference of 12.5 kcal·mol^{-1} can be taken as the strain energy of deformation of **1a**, due to the Me-crowding effect in **1a**. Indeed, the calculated ΔH_f° value for **1b** (-20.18 kcal·mol^{-1}) deviates only slightly (by 0.26 kcal·mol^{-1}) from the value estimated by the described incremental procedure (-20.44 kcal·mol^{-1}), indicating that **1b** is free of group-crowding strain.

On the other hand, the HOMO, LUMO, and NLUMO coefficients of **1a**–**1c** are as expected quite similar (*cf. Fig. 4*) [4] (*cf.* also [1]). They should admit at least two different types of orbital-symmetry controlled, thermal reactions, namely a first-order transformation, steered by the HOMO of **1**, which will result in disrotatory ring closure by bond formation between C(3a) and C(8) as well as a second-order [8+2] cycloaddition reaction between two molecules of **1**, governed by HOMO-LUMO interactions. Despite the fact that **1a** is formed by vacuum flash pyrolysis of (2,3,4,5,6-pentamethyl)phenyl prop-2-ynoate at *ca.* 650° [2], it may undergo in solution, due to its Me-crowding strain, intramolecular ring closure to **7a**, which can relieve strain by homolysis of the O–C bond. The thus formed diradical **8a** may then undergo a

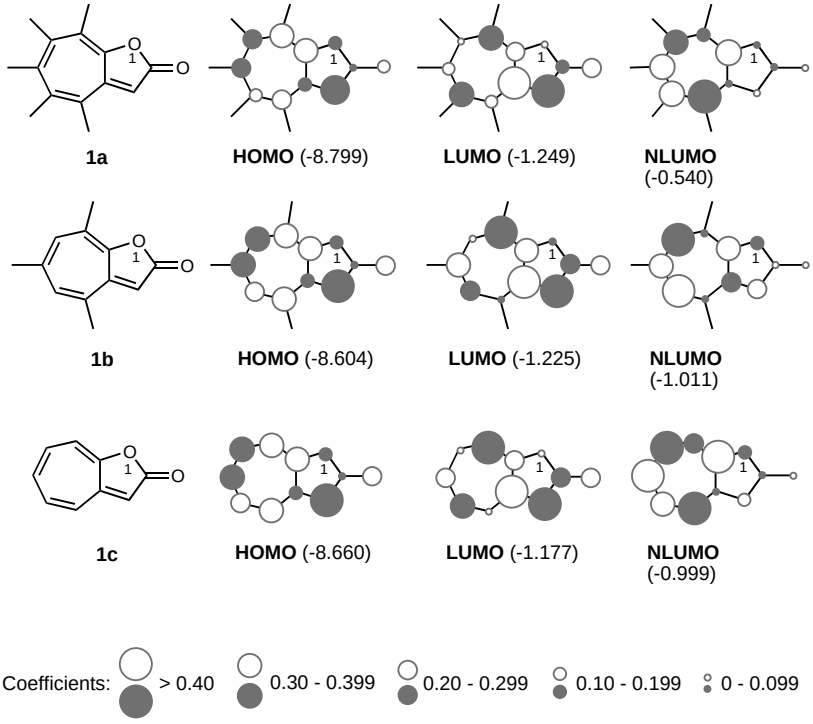

Fig. 4. *HOMO, LUMO, and NLUMO coefficients of the* 2H-*cyclohepta*[b]*furan-2-ones* **1a**–**c** (taken from [4]; geometry optimization with 'Gaussian-94'; semi-empirical calculations with MNDO)

fragmentation reaction under extrusion of CO_2 and formation of 1-ethynyl-2,3,4,5,6-pentamethylbenzene (**9a**) (*cf. Scheme 4*). The latter compound could add in a [8 + 2] fashion to **1a** (*cf.* [4]). Loss of CO_2 from the cycloadduct **10a** would finally yield **4a**. We studied this reaction sequence by thermal reaction of independently synthesized **9a** with **1a** in decalin at 190°. However, the only product that was isolated in 89% yield, after 15 h heating, was the [4 + 2] cycloadduct **11a**. This result demonstrates that the discussed reaction sequence (*cf. Scheme 4*) cannot be responsible for the formation of the main product **4a**.

The [8 + 2] cycloaddition reaction between two molecules of **1a** follow, in principle, the normal reactivity of 2*H*-cyclohepta[*b*]furan-2-ones in the presence of electron-donor substituted ethenes, with the sole difference that a second molecule of **1a** takes the part of the electron-donor substituted ethene. Four different transition-state arrangements of the two molecules of **1a** are thinkable, resulting in four diastereoisomeric dimers **12a**, which may be named according to the relative orientation of the two C=O groups *syn* or *anti* and *exo* or *endo* with respect to the relative position of the anellated furanone ring at the formed central 2-oxanorbornan-3-one substructure. The AM1-calculated structures of the four possible diastereoisomers of **12a** are displayed together with their calculated ΔH_f° values in *Fig. 5*. The enthalpy of formation of two mol of **1a** amounts to $2 \cdot (-22.16\ \text{kcal} \cdot \text{mol}^{-1}) = -44.32\ \text{kcal} \cdot \text{mol}^{-1}$, which demon-

Scheme 4

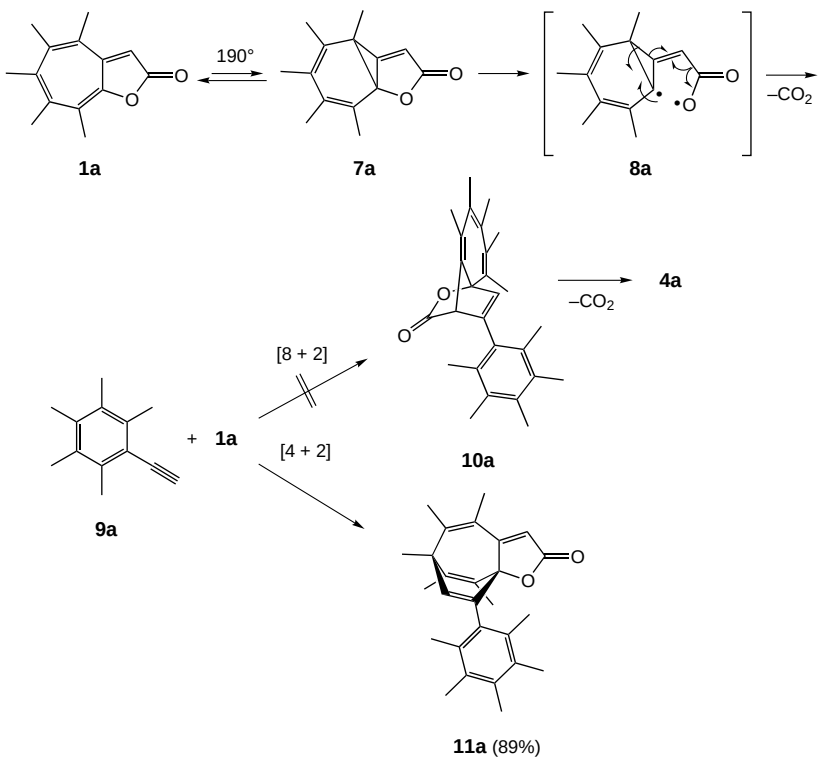

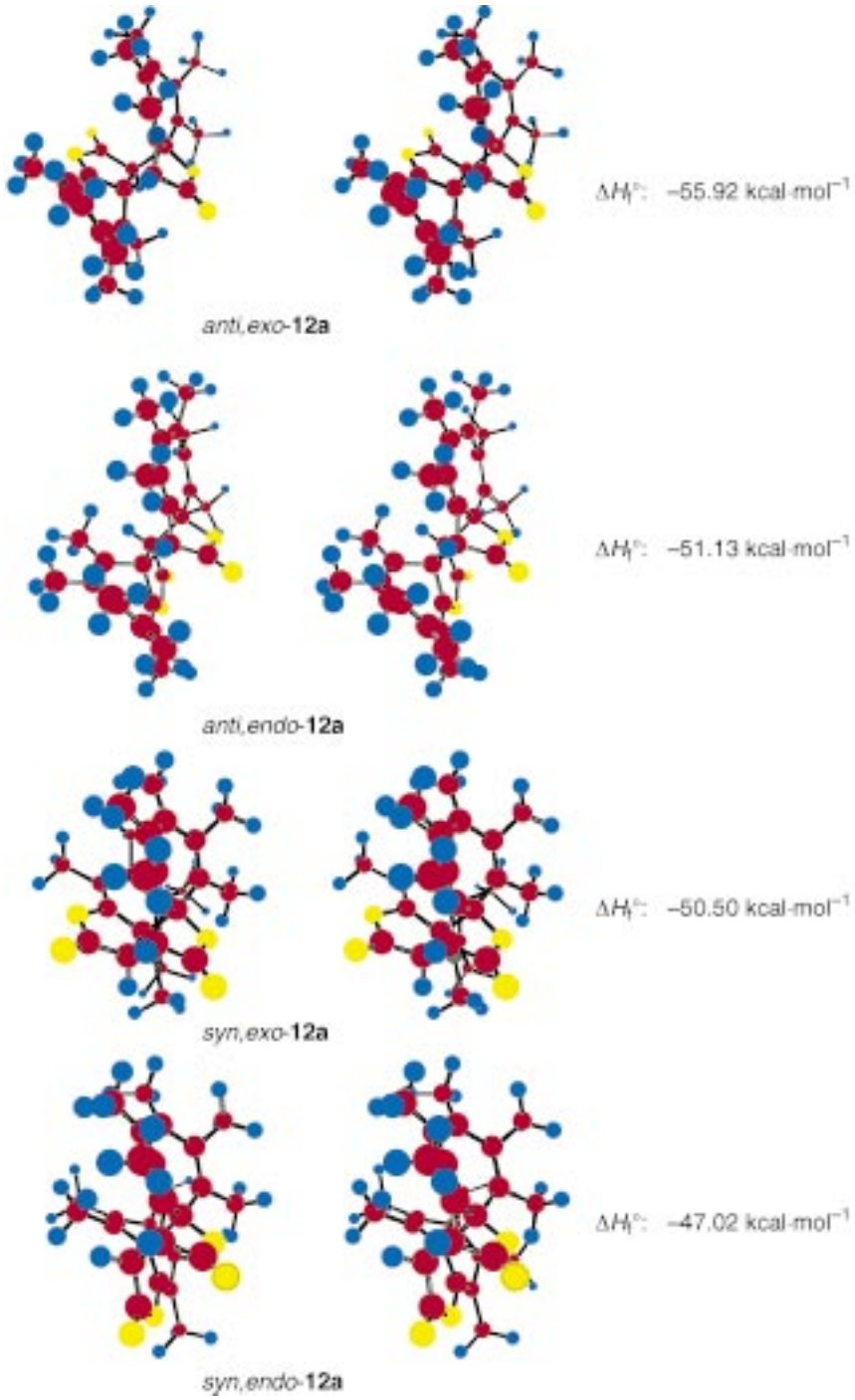

Fig. 5. *Stereoscopic view of the AM1-calculated structures of the four possible [8 + 2] cycloaddition products of* **1a**, C = magenta, H = blue, O = yellow.

strates that all four cycloaddition reactions are possible, whereby the formation of *anti*,*exo*-**12a** is most favorable with a gain in enthalpy of 11.60 kcal · mol^{-1}. The next step, to be expected according to the known cycloaddition/cycloreversion chemistry of 2*H*-cyclohepta[*b*]furan-2-ones, should be the extrusion of CO_2 from the 2-oxanorbornan-3-one part of **12a**. The steps leading finally to **4a** are displayed in *Scheme 5*, and the corresponding AM1-calculated structures are shown in *Fig. 6*. At a certain stage of the transformations, ring contraction of one of the seven-membered rings to the (pentamethylphenyl)-substituent has to take place. This normally happens in heptalene chemistry *via* the cycloheptatriene ⇌ norcaradiene equilibrium, followed by cleavage of one of the 'old' cyclopropane bonds (*cf.* [6][7] as well as *Sect. 3*). We believe that in the present case, intermediate **13a** undergoes ring contraction with its cycloheptatriene ring B, which possesses, in contrast to ring A, the shorter C,C distance for bond formation (ring B, 247 pm, and ring A, 255 pm) due to the larger torsion angles along its conjugated triene system. The $\Delta\Delta H_f^\circ$ value of **13a** and its ring-closed form **14a** amounts to 18.37 kcal · mol^{-1} (*cf. Fig. 6*), *i.e.*, does not forbid the ring-closure reaction. Homolysis of the cyclopropane bond that includes C(2) of the 1,2-dihydroazulene substructure creates a strain-relaxed highly delocalized diradical **15a**, which, on loss of CO_2, concerted or non-concerted stepwise, gives **4a** in an overall strongly exothermic reaction (*cf. Fig. 6*). The dimer *anti*,*endo*-**12a** (*cf. Fig. 5*), which lies by 4.79 kcal · mol^{-1} higher in ΔH_f° than *anti*,*exo*-**12a** will also give **13a** on loss of CO_2, so that it also may take part to a certain extent in the formation of **4a**. However, the discussed reaction sequence, applied to the other two dimers of **12a**, with *syn* orientation of the two C=O groups and the two seven-ring systems, therefore higher lying in ΔH_f° than the two *anti*-forms of **12a** (*cf. Fig. 5*), would lead finally to 4,5,6,7,8-pentamethyl-1-[(2,3,4,5,6-pentamethyl)phenylazulene, an isomer of **4a**, which was not observed.

The failure of the other 2*H*-cyclohepta[*b*]furan-2-ones to undergo the reactions observed with **1a** as well as the successful cross experiments with **1b** and **1c** (*cf. Scheme 3*) are in full agreement with this sketched reactivity of **1a**. The formation of the azulenes **4ba** and **4ca**, respectively, in the cross reactions clearly indicate, on the basis of the postulated *Scheme 5* and *Figs. 5* and *6*, that **1a** entered the cycloaddition

Scheme 5

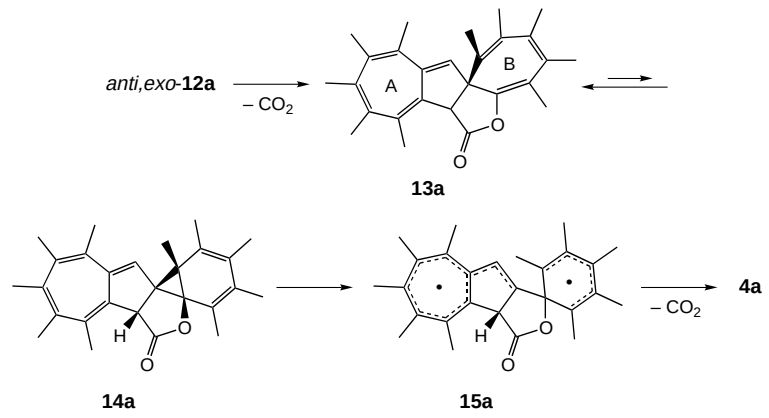

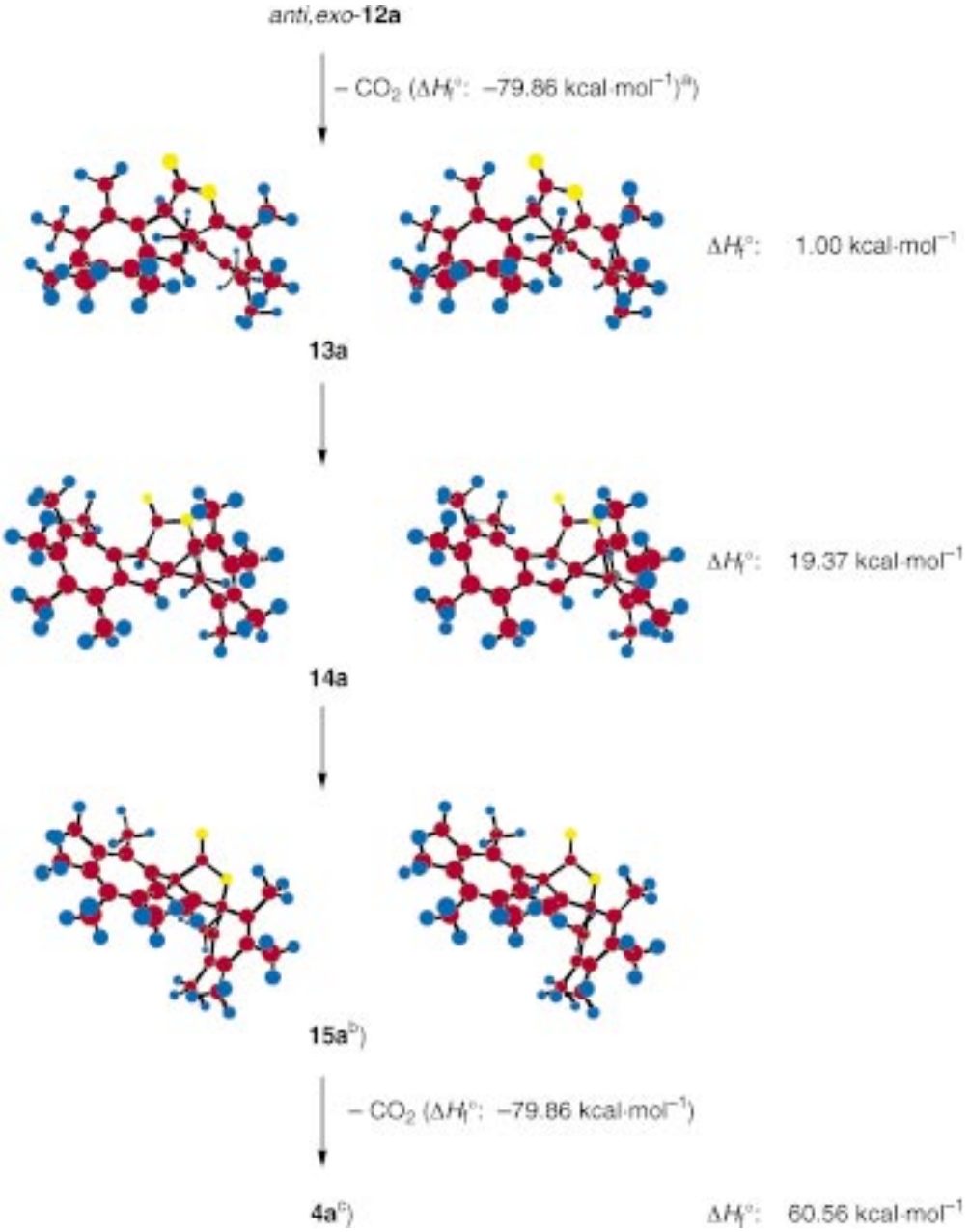

Fig. 6. *Stereoscopic view of the calculated structures of the intermediates* **13a**, **14a** (AM1), *and the* π_2*-diradical* **15a** (MM2; *cf. Scheme 5*) *on the postulated reaction path of* anti,exo-**12a** *to* **4a**. For colors, see *Fig. 5*

reaction as 2-atom component, whereas **1b** or **1c** acted as its 8-atom reaction partner. The other two possible azulenes **4ab** and **4ac**, respectively, with exchanged azulene and phenyl part were not observed in the corresponding reaction mixtures. *Table 3* contains the AM1-calculated ΔH_f° values of all *anti*-intermediates **12** of the cycloaddition reactions of **1**, including the cross reactions of **1a** with **1b** or **1c**. The relevant structures of *anti*,*exo*-**12ba** and *anti,exo*-**12ca** that will lead to the observed 'cross' azulenes **4ba** and **4ca**, respectively, are displayed in *Fig. 7*.

Table 3. *Comparison of the AM1-Calculated* ΔH_f° *Values of the Possible* anti-*Addition Products* **12** *of the* 2H-*Cyclohepta*[b]*furan-2-ones* **1**[a])

Addition products **12**	Calculated ΔH_f°	Sum of ΔH_f° of starting **1**	Gain in ΔH_f° of **12** ($\Delta\Delta H_f^\circ$)[b])
anti,*exo*-**12a**[c])	– 55.92	– 44.32	11.60
anti,*exo*-**12b**	– 45.03	– 40.36	4.67
anti,*exo*-**12c**	– 6.36	– 1.12	5.24
anti,*exo*-**12ab**[d])	– 48.00	– 42.34	5.66
anti,*exo*-**12ba**[d])	– 52.65	– 42.34	10.31
anti,*exo*-**12ac**[d])	– 28.72	– 22.72	6.00
anti,*exo*-**12ca**[d])	– 33.77	– 22.72	11.05
anti,*endo*-**12a**[c])	– 51.13	– 44.32	6.81
anti,*endo*-**12b**	– 43.00	– 40.36	2.64
anti,*endo*-**12c**	– 4.90	– 1.12	3.78
anti,*endo*-**12ab**[d])	– 43.10	– 42.34	0.76
anti,*endo*-**12ba**[d])	– 51.05	– 42.34	8.71
anti,*endo*-**12ac**[d])	– 24.15	– 22.72	1.43
anti,*endo*-**12ca**[d])	– 32.00	– 22.72	9.28

[a]) ΔH_f° and $\Delta\Delta H_f^\circ$ in kcal · mol^{-1}. [b]) Underlined $\Delta\Delta H_f^\circ$ values belong to the reaction sequence of the observed azulenes **4**. [c]) See *Fig. 5*. [d]) The first letter indicates the component **1** that will become in the course of the reaction the azulene part; the second letter stands for the component **1** that will become later the phenyl substituent at C(2) of the formed azulene ring.

It is striking that all postulated *anti*-intermediates **12** that should lead, according to *Scheme 5*, to the observed azulenes **4a**, **4ba**, and **4ca** exhibit indeed the largest gain in enthalpy in comparison to the sum of ΔH_f° of the starting 2*H*-cyclohepta[*b*]furan-2-ones **1**, whereby the *anti*,*exo*-diastereoisomers of **12** possess in all cases the larger difference than the corresponding *anti*,*endo*-diastereoisomers. The $\Delta\Delta H_f^\circ$ values for *anti*,*exo*-**12b** and -**12c** in comparison to that of *anti*,*exo*-**12a** also explain why pure **1b** and **1c**, respectively, do not undergo the dimerization reaction under the applied conditions. The gain in enthalpy ($\Delta\Delta H_f^\circ$) is well below 10.3 kcal · mol^{-1}, which is the lowest for the cycloaddition reaction that finally gives **4ba**. Moreover, this value is by 0.74 kcal · mol^{-1} lower than that for the formation of *anti*,*exo*-**12ca**. The results are in full accord with these findings, since **4ca** is already formed as the major azulene when equimolar amounts of **1a** and **1c** are reacted, whereas the formation of **4ba** as major azulene requires a 3-fold molar amount of **1b** in the presence of 1 mol-equiv. of **1a**. The conclusion is that in crossed cycloaddition reactions of **1a** with other 2*H*-cyclohepta[*b*]furan-2-ones, **1a** is an equivalent for the introduction of the (2,3,4,5,6-pentamethyl)phenyl substituent at C(2) of azulenes, with a substitution pattern at the seven-membered ring that is determined by the other component **1**. The reason for this

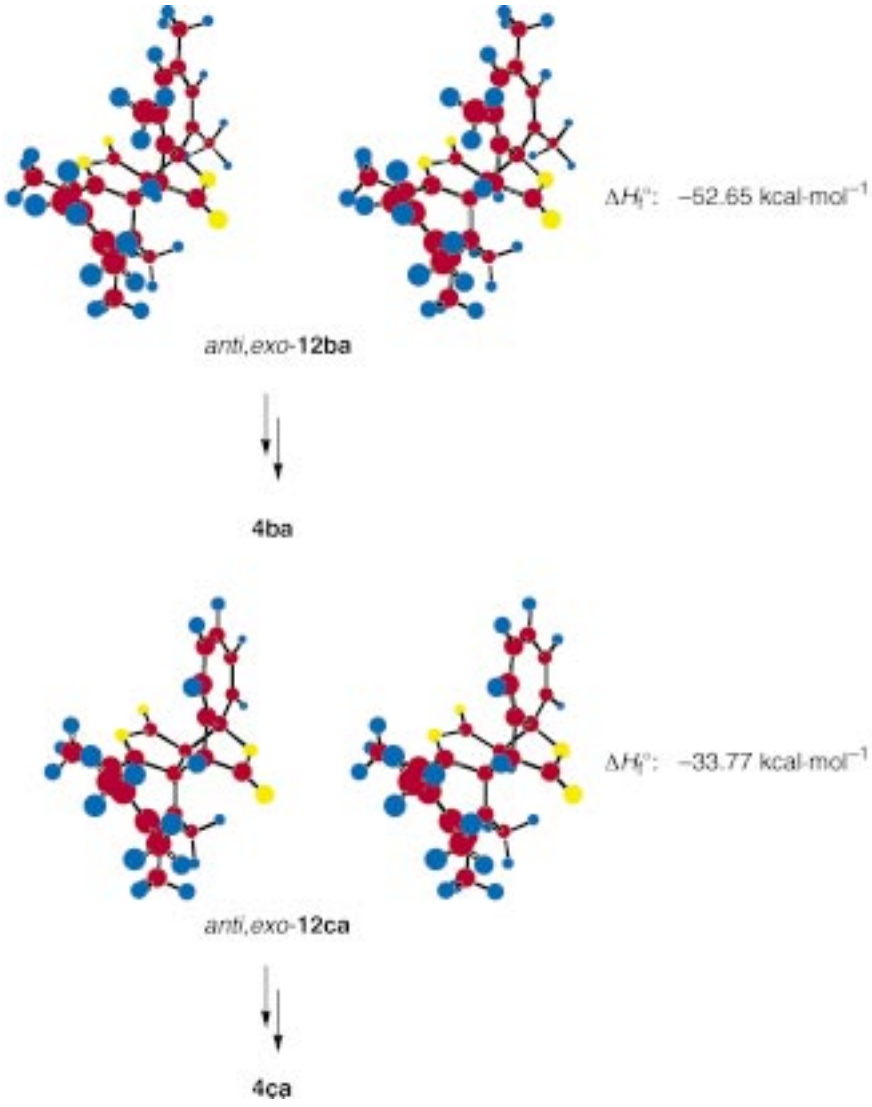

Fig. 7. *Stereoscopic view of the AM1-calculated structures of the energetically most favorable [8+2]* anti,exo-*cycloadducts* **12ba** *and* **12ca**, *leading to the 'mixed' azulenes* **4bc** *and* **4ca**, *respectively* (for colors, see *Fig. 5*)

chemoselectivity is apparent. The Me-crowding energy of **1a** (*vide supra*) is best reduced in the transition state of the cycloaddition reaction when **1a** takes part as 2-atom component, which leads to a cycloadduct **12** where the seven-membered ring of **1a** becomes the strongly puckered cycloheptatriene ring, which is spiro-linked to the central 2-oxanorban-3-one unit. The other cycloheptatriene ring, which is anellated to this central unit along the C(1)–C(7) bond, is forced in a planar conformation due to the bicyclo[2.2.1] nature of the central unit.

We believe that the central diradical **15a** is also responsible for the formation of the pentamethylazulene **5a** as well as for the indene **6a** in the thermal reaction of **1a**. Intramolecular disproportionation of **15a** *via* 1,4-H transfer will lead to the intermediate **16a** (*Scheme 6*). The AM1-calculated ΔH_f° value of **16a** (4.29 kcal · mol^{-1}) is close to that of the precursor **14a**, which amounts to 1.00 kcal · mol^{-1}. Concerted – in the sense of a linear cheletropic fragmentation – or non-concerted, *via* stepwise homolysis, loss of CO_2 will give azulene **5a** and the benzyl-phenyl-centered diradical **17a**, which may also be formulated as a 6-methylidenecyclohexa-2,4-dien-1-ylidene. It seems that **17a** is trapped by **1a**, but neither by **1b** nor **1c** in the cross experiments, in a [2 + 3] 6e-cycloaddition reaction resulting in the formation of **18a**[2]). The concertedness of [2 + 3] cycloaddition reactions with singulet 1,3-diradicals and alkenes is well-established (see, *e.g.*, [8]). As an intermediate with a cycloheptatriene substructure, **18a** may undergo intramolecular disrotatory ring closure to **19a**. This intermediate possesses again the possibility of a concerted or non-concerted, stepwise extrusion of CO_2 under cleavage of one of the 'old' cyclopropane bonds and formation of the 1*H*-indene derivative **6a**.

3. Heptalene Formation. – The thermal reaction of the 2-(pentamethylphenyl)-substituted azulenes **4a** and **4ba** and the pentamethyl-substituted heptalene **5a** with an excess of dimethyl acetylenedicarboxylate (ADM) in toluene gave in all three cases the expected heptalenedicarboxylates as a mixture of their double-bond-shifted (DBS) isomers (*Scheme 7*). Small amounts of the corresponding azulene-1,2-dicarboxylates **21** and **23** were also formed, as it is generally observed for thermal reactions of azulenes

Scheme 6[a])

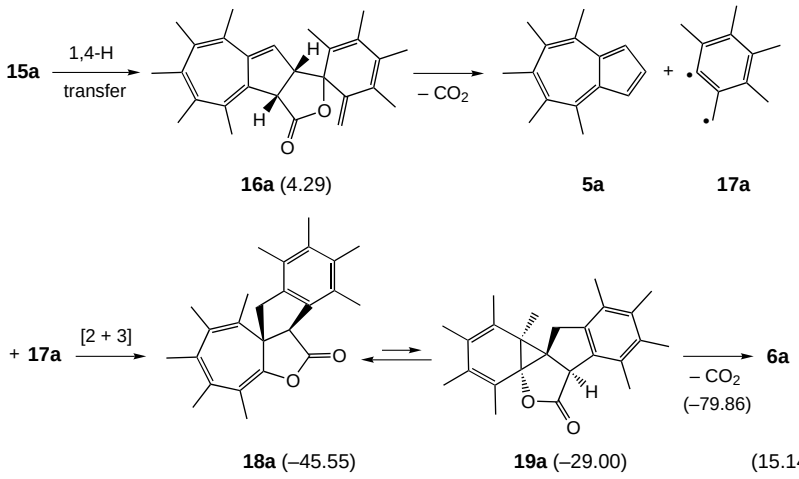

[a]) In parentheses, AM1-calculated ΔH_f° values in kcal · mol^{-1}.

[2]) The product resulting from the reverse regioselectivity may also be formed. However, its ΔH_f° value is, according to AM1 calculations, by more than 10 kcal · mol^{-1} higher than that of **18a**, which makes its formation unlikely. Nevertheless, its transformation, following *Scheme 6*, will also lead to **6a** and **17a**, due to the pseudo-symmetry plane of **6a**.

Scheme 7[a])

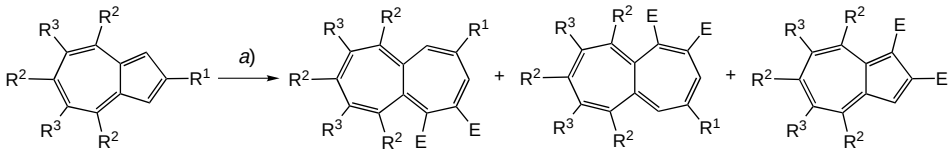

5a R^1 = H, R^2 = R^3 = Me — **20** (16%) — **20'** — **21** (<1%)

4ba R^1 = PMP, R^2 = Me, R^3 = H — **22** (34%) — **22'** — **23** (9%)

4a R^1 = PMP, R^2 = R^3 = Me — **24** (39%) — **24'** — **21** (<1%)

25 (n.o.)

26 (n.o.)

27 (3%)

a) 4–8 mol-equiv. of ADM; toluene, 130°, 10–1800 min.

[a]) For details, see *Exper. Part*.

with ADM (*cf.* [9–11]). The total yield of the DBS mixture of the pentamethylheptalenedicarboxylates **20**/**20′** was distinctly lower than those of the heptalenedicarboxylates **22**/**22′** and **24**/**24′** with the (pentamethylphenyl) group at C(2)/C(4) due to the fact that azulene **5a** is thermally much less stable (*cf.* [1]) than the azulenes **4a** and **4ba** with the (pentamethylphenyl) residue at C(2).

The thermal reaction of **4a** and ADM gave, as further product, the acenaphthylene-3,4-dicarboxylate **27** (*Scheme 7*). It must have been formed by a similar mechanism as other products of this type (*cf.* [5][6]). However, in contrast to our former findings, where dehydrogenation or leaving-group elimination has to take place in the final step of aromatization, we have to assume that in the present case, methane is split off (*Scheme 8*). The formation of analog products (**25** or **26**) were not observed in the two

Scheme 8

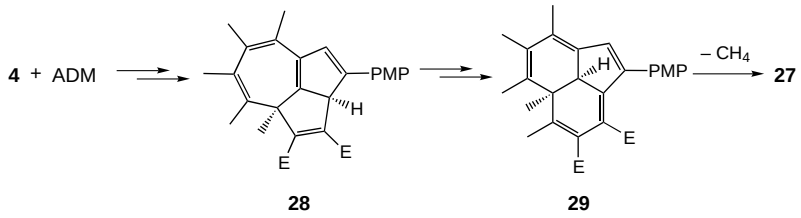

other thermal reactions. The structure of **27** was solved unambiguously by an X-ray crystal-structure determination (see *Exper. Part*).

All new heptalenedicarboxylates could easily be equilibrated thermally (*cf. Scheme 9*). The DBS process could also be induced photochemically (see *Exper. Part*). The thermal equilibrium ratios of the heptalenedicarboxylates do not differ very much. It seems, however, that the Me_5 substitution pattern as in **20**/**20′** or **24**/**24′** favors the 4,5-dicarboxylate structures slightly more than the 6,8,10-Me_3 pattern as present in **22**/**22′** or **30**/**30′**, in agreement with corresponding AM1 calculations of ΔH_f°, whereby the (pentamethylphenyl) or a phenyl substituent at C(2)/C(4) has no significant influence on the equilibrium ratios. The two Me substitution patterns have a much stronger impact on the rate ($k_1 + k_{-1}$) of the equilibration process. One observes an expressed buttressing effect of the 5 adjacent Me groups in **20**/**20′** and **24**/**24′** in comparison with the 3 non-adjacent Me groups in **22**/**22′** and **30**/**30′**. The two DBS isomers **24** and **24′** are thermally stable enough at room temperature that both isomers can be separated by chromatography. Similarly, the ratio of the photo-equilibrium mixture **20**/**20′** (54 : 46; see *Exper. Part*) is thermally not altered at room temperature. First kinetic experiments in toluene gave for **24**/**24′** a total half-life ($\tau_{1/2}$(**24**) + $\tau_{1/2}$(**24′**)) of *ca.* 45 min and for **20**/**20′** of *ca.* 22 min at 100°. In contrast to these findings, pure crystalline **22** equilibrates already on dissolution in toluene at room temperature, so that we were not able to measure the kinetics of equilibration under our standard conditions. The same is true for **30**/**30′** (*cf.* [12]).

Scheme 9[a])

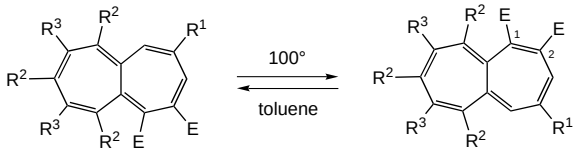

20	90 : 10	**20'**
22	74 : 26	**22'**
24	84 : 16	**24'**
30	77 : 23[b])	**30'**

[a]) R^1 to R^3, see *Scheme 7* and *Table 5* for **30**; equilibrium ratios in %. [b]) Hexane, 20° [12].

The structure of the 2-(pentamethylphenyl)-substituted heptalene-4,5-dicarboxylates **22** and **24** were ascertained by X-ray crystal-structure analyses (see *Exper. Part* and *Tables 4* and *5*). The crystals of **24** exhibited unfortunately twinned regions[3]). The structure refinement was, therefore, distinctly worse than that of **22**, which gave standard *R* values. Nevertheless, the structure of **24** and its relative configuration was clearly solved (*cf. Fig. 8*). A comparison of the skeletal torsion angles Θ of **22** and **24**

[3]) A number of further attempts to crystallize **24** did not improve the quality of the crystals due to the fact that **24** is highly soluble in all common organic solvents, so that only hexane was left for crystallization experiments.

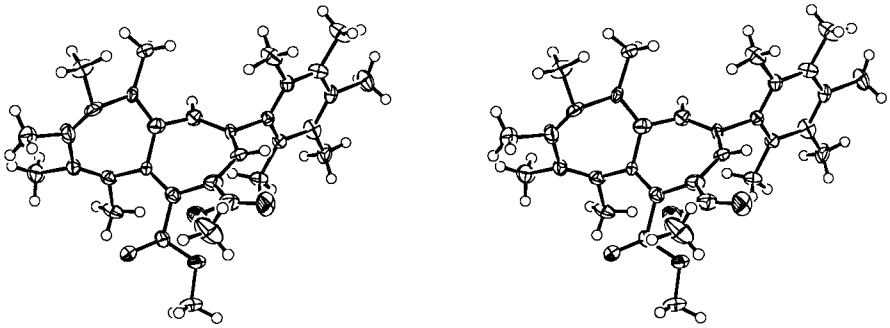

Fig. 8. *Stereoscopic view of the X-ray crystal structure of the sterically most crowded 4,5,6,7,8-pentamethyl-2-(2,3,4,5,6-pentamethylphenyl)azulene* (**24**)

Table 4. *Comparison of Some X-Ray Crystal-Structure Data of the Heptalene-4,5-dicarboxylates* **22**, **24**, *and* **30**[a])

	22	**24**	**30**
Bond angles ϑ [°]:			
C(1)–C(10a)–C(5a)	113.5(2)	116.4(10)	115.1(1)
C(5)–C(5a)–C(10a)	121.5(2)	121.2(9)	121.8(1)
C(5a)–C(10a)–C(10)	123.7(2)	124.1(10)	122.7(1)
C(6)–C(5a)–C(10a)	113.0(2)	113.3(10)	114.4(1)
C(7)–C(8)–C(9)	124.3(3)	125.2(9)	123.0(1)
Torsion angles Θ [°]:			
C(4)–C(5)–C(5a)–C(6)	178.5(2)	172.3(9)	172.8(1)
C(5)–C(5a)–C(6)–C(7)	123.5(3)	127.5(11)	120.2(1)
C(5)–C(5a)–C(10a)–C(10)	– 122.7(3)	– 125.4(11)	– 123.6(1)
C(1)–C(10a)–C(5a)–C(6)	– 116.9(3)	– 115.2(10)	– 114.4(1)
C(1)–C(10a)–C(10)–C(9)	173.6(3)	– 179.7(10)	175.3(1)
C(10)–C(10a)–C(1)–C(2)	121.7(3)	127.7(12)	124.3(1)
C(3)–C(4)–C(1″)=O	– 178.1(3)	– 21.5(17)	– 25.1(2)
C(5a)–C(5)–C(1‴)=O	– 44.4(4)	– 31.6(16)	154.8(1)
C(2)–C(3)–C(4)–(1″)	177.7(3)	– 177.8(10)	– 176.2(1)
C(1‴)–C(5)–C(5a)–C(10a)	– 176.6(2)	– 176.8(9)	– 75.6(1)
C(1)–C(2)–C(1′)–C(2′)	86.9(3)	85.6(12)	31.2(2)
C(1″)–C(4)–C(5)–C(1‴)	– 37.5(3)	– 40.5(14)	– 41.6(2)

[a]) The quality of the crystals of **24** could not be improved by recrystallization. For heptalenedicarboxylate **30**, see *Table 5*.

and of heptalene-4,5-dicarboxylate **30** as the phenyl analog of **22** (see *Tables 4* and *5*) shows that all three heptalene-4,5-dicarboxylates possess in the crystals similar Θ at the MeOCO-substituted ring as well as at the central σ-bond, common for both rings. It seems that an average Θ value of $60-61^\circ$ at the central σ-bond represents the utmost size that is structurally possible by the anellation of two seven-membered, fully unsaturated rings. The central Θ values of **24** as the sterically most encumbered heptalene-4,5-dicarboxylate fall exactly in this range. The steric congestion of the 5 adjacent Me groups of **24** is compensated by the peripheral torsion angles of the seven-

Table 5. *Torsion Angles Θ from X-Ray Crystal Structure Analyses of the 2-(Pentamethylphenyl)-Substituted Heptalene-4,5-dicarboxylates* **22** *and* **24** *in Comparison with Those of the 2-Phenyl Analog* **30** *of* **22**

	Heptalene-4,5-dicarboxylate[a])		
	22	**30**[b])	**24**[c])
s-*cis*-Buta-1,3-diene subunits torsion angles Θ [°]:			
C(1)–C(2)–C(3)–C(4)	38.3(5)	31.4(2)	37.2(15)
C(3)–C(4)–C(5)–C(5a)	– 39.5(4)	– 36.9(2)	– 36.3(16)
C(6)–C(7)–C(8)–C(9)	34.0(5)	34.1(2)	48.3(19)
C(8)–C(9)–C(10)–C(10a)	– 29.8(5)	– 34.4(2)	– 37.4(18)
cis-Ethene subunits torsion angles Θ [°]:			
C(2)–C(3)–C(4)–C(5)	0.4(5)	4.5(2)	1.2(18)
C(10a)–C(1)–C(2)–C(3)	– 1.9(5)	1.1(2)	– 5.5(16)
C(5a)–C(6)–C(7)–C(8)	2.9(5)	5.6(2)	7.8(16)
C(7)–C(8)–C(9)–C(10)	– 2.2(5)	– 1.5(2)	6(2)
Central σ-bond *cisoid* torsion angles Θ [°]:			
C(10a)–C(1)–C(2)–C(3)	59.3(4)	60.7(2)	58.0(13)
C(10a)–C(1)–C(2)–C(3)	61.2(4)	61.4(2)	61.4(13)

[a]) Torsion angles Θ are given for the (*P*)-configuration. [b]) Data for **30** are taken from [12];

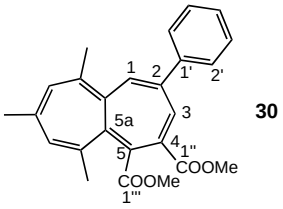

30

[c]) The large e.s.d. values are due to the bad quality of the crystals of **24**, which could not be improved despite several recrystallizations.

membered ring that carries the Me groups. Its torsion angles at the s-*cis*-buta-1,3-dienyl subunits are in average 10° larger than those at the 6,8,10-Me_3 substituted rings in **22** and **30**. The transition state of the DBS process in heptalenes must be still twisted since it occurs with retention of the configuration of the inherently chiral heptalene skeleton [13] (see also [14]). Therefore, we have to expect that adjacent Me groups will come closer in the transition state since all peripheral torsion angles will be reduced in the transition state to allow the cyclic π-bond jump from one DBS isomer to the other[4]).

Finally, it is worthwhile to mention that the ^{1}H- and ^{13}C-NMR spectra of **22** and **24** and their DBS isomers **22′** and **24′** indicate a restricted rotational freedom of the 2-

[4]) Similar observations have been made by *Paquette et al.* for the cyclic π-bond shift in highly methylated cyclooctatetraenes (see [15] and ref. cit. therein). DFT Calculations that we have performed on heptalenes [16], partly in cooperation with Prof. *W. Thiel* and Dr. *E.-U. Wallenborn*, show that the lowest excited state of heptalenes is still twisted, however, with equalized bond lengths. Therefore, we believe that the DBS process in heptalene is characterized by touching of the hypersurfaces of the ground and excited singlet state, in agreement with all our experiments, especially with respect to the observed retention of configuration in thermally or photochemically induced DBS in optically active heptalenes [13]. We will come back to this point in a planned publication [16].

(pentamethylphenyl) substituents, in a way that all four forms exhibit 5 sharp *s* for the 5 aromatically bound Me groups due to the inherent chirality of the heptalene skeleton.

We thank Dr. *H. W. Schmalle*, Anorganisch-chemisches Institut der Universität Zürich, and Dr. *A. Linden* for the X-ray crystal-structure determinations, Dipl.-Chem. *M. Nagel* for the arrangement of *Fig. 4*, our NMR laboratory, in particular *Nadja Walch* and Dr. *Gudrun Hoppe*, for specific NMR measurements, Prof. *M. Hesse* and his group for mass-spectrometric measurements, and our Analytical Laboratory for elemental analyses. The financial support of this work by the *Swiss National Science Foundation* is gratefully acknowledged.

Experimental Part

General. HPLC: *Bischoff* HPLC pump model *2200* with an anal. column *Spherisorb Nitrile* (3 μm, 10 × 3 mm); photodiode array detector (*Waters 991*). Prep. HPLC: *Du Pont Instruments-830* liquid chromatograph; prep. column (250 × 20 mm) with the stationary phase *Spherisorb S5 CN*. UV Spectra: *Perkin-Elmer Lambda-19* spectrometer, λ_{max} (log ε) in nm. IR Spectra: *Perkin-Elmer Spectrum-One* spectrometer; in cm^{-1}. ^{1}H- and ^{13}C-NMR Spectra: *Bruker* instruments *ARX-300* (300 and 75 MHz, resp.), *Avance DRX-500* (500 and 125 MHz, resp.), and *Avance DRX-600* (600 and 150 MHz, resp.); chemical shifts δ in ppm rel. to $CD(H)Cl_3$ (7.270 and 77.00 ppm, resp.); complete assignments of ^{1}H signals by COSY, TOCSY, NOESY, ROESY 2D or 1D NMR methods; complete assignments of ^{13}C-signals by 2D HMBC and HSQC methods. Electron-impact (EI) MS: *Finnigan SSQ-700* mass spectrometer. Chemical-ionization (CI) MS: *Varian MAT-90* mass spectrometer, ionization *via* methane.

*2*H-*Cyclohepta[*b*]furan-2-ones* **1a**–**c** were synthesized according to [1]. The 4,5,6,7,8-pentafluoro-2*H*-cyclohepta[*b*]furan-2-one (**1d**) was prepared according to a published procedure [17]. All reactions were performed under Ar.

1. *Azulenes by Thermolysis of 2*H-*Cyclohepta[*b*]furan-2-ones* **1**. 1.1. *Thermolysis of 4,5,6,7,8-Pentamethyl-2*H-*cyclohepta[*b*]furan-2-one* (**1a**). A soln. of **1a** (1.3 g, 6.01 mmol) in decalin (10 ml) was flushed with Ar in a *Schlenk* vessel. The vessel was closed and heated at 230–240° during 3.5 h. The solvent was evaporated. The residual black solid was then immediately chromatographed on a short column (Al_2O_3, gradient hexane → CH_2Cl_2/acetone 90 : 10) to separate the blue azulene fraction (390 mg) from starting material (0.113 g, 9%) and polymeric stuff. The subsequent CC (silica gel, hexane) of the azulene fraction gave **4a** (0.269 g, 26%), **5a** (0.06 g, 10%), and **6a** (0.06 g, 6%).

Data of 4,5,6,7,8-Pentamethyl-2-(2,3,4,5,6-pentamethylphenyl)azulene (**4a**): Light blue crystals. M.p. 272.3–272.7° (hexane). UV/VIS (hexane; *cf. Fig. 2*): 566 (2.76), 370 (sh, 3.48), 360 (3.74), 351 (sh, 3.70), 304 (4.64), 255 (4.29), 247 (sh, 4.23), 200 (4.77); min. 425 (2.08), 339 (3.65), 267 (4.02), 232 (4.20). ^{1}H-NMR (500 MHz, C_6D_6): 7.30 (*s*, H–C(1,3)); 2.62 (*s*, Me–C(4,8)); 2.28 (*s*, Me–C(2′,6′)); 2.25 (*s* Me–C(4′)); 2.23 (*s*, Me–C(3′,5′)); 2.18 (*s*, Me–C(6)); 2.15 (*s*, Me–C(7,5)). ^{13}C-NMR (125 MHz, $CDCl_3$): 150.12 (*s*, C(2)); 144.13 (*s*, C(6)); 143.36 (*s*, C(4,8)); 139.29 (*s*, C(3a,8a)); 138.56 (*s*, C(1′)); 133.64 (*s*, C(4′)); 132.33 (*s*, C(3′,5′)); 132.26 (*s*, C(2′,6′)); 130.98 (*s*, C(5,7)); 116.28 (*d*, C(1,3)); 24.72 (*q*, *Me*–C(6)); 22.99 (*q*, *Me*–C(5,7)); 22.86 (*q*, *Me*–C(4,8)); 19.63 (*q*, *Me*–C(2′,6′)); 17.19 (*q*, *Me*–C(4′)); 17.13 (*q*, *Me*–C(3′,5′)). EI-MS: 344.2 (100, $M^{+\cdot}$), 329.2 (49, $[M-Me]^+$), 314.1 (84, $[M-2\,Me]^+$), 299.1 (55, $[M-3\,Me]^+$). Anal. calc. for $C_{26}H_{32}$ (344.53): C 90.64, H 9.36; found: C 90.34, H 9.44.

Data of 4,5,6,7,8-Pentamethylazulene (**5a**): Blue crystals. M.p. 86.3–93.1° (hexane). UV/VIS (hexane; *cf. Fig. 1*): 574 (2.78), 366 (sh, 3.46), 356 (3.46), 344 (sh, 3.60), 294 (4.57), 252 (4.38), 200 (4.21); min 420 (2.10), 330 (2.52), 266 (4.00), 224 (4.04). ^{1}H-NMR (300 MHz, C_6D_6): 7.64 (*t*, $^3J(2,1) = {}^3J(2,3) = 4.0$, H–C(2)); 7.27 (*d*, $^3J(1,2) = {}^3J(3,2) = 4.0$, H–C(1,3)); 2.45 (*s*, Me–C(4,8)); 1.94 (*s*, Me–C(6)); 1.92 (*s*, Me–C(5,7)). ^{13}C-NMR (150 MHz, $CDCl_3$): 145.30 (*s*, C(6)); 144.34 (*s*, C(4,8)); 137.53 (*s*, C(3a,8a)); 132.29 (*d*, C(2)); 130.44 (*s*, C(5,7)); 114.10 (*d*, C(1,3)); 24.72 (*q*, *Me*–C(6)); 22.96 (*q*, *Me*–C(5,7)); 22.77 (*q*, *Me*–C(4,8)). EI-MS: 198.0 (95, $M^{+\cdot}$, $C_{15}H_{18}^{+\cdot}$), 183.0 (100, $[M-Me]^+$).

*Data of 4,5,6,7-Tetramethyl-2-(2,3,4,5,6-pentamethylphenyl)-1*H-*indene* (**6a**): Colorless crystals. M.p. 280.0–282.8° (hexane). UV (hexane): 272 (4.11), 220 (sh, 4.44), 202 (4.67); min. 249 (3.83). ^{1}H-NMR (500 MHz, $CDCl_3$): 6.72 (*s*, H–C(3)); 3.46 (*s*, 2 H–C(1)); 2.41 (*s*, Me–C(4)); 2.31 (shoulder of *s*, Me–C(7)); 2.30 (*s*, Me–C(5), Me–C(6), Me–C(4′)); 2.67 (*s*, Me–C(3′), Me–C(5′)); 2.15 (*s*, Me–C(2′), Me–C(6′)). ^{13}C-NMR (125 MHz, $CDCl_3$): 147.63 (*s*, C(2)); 141.60 (*s*, C(3a)); 139.47 (*s*, C(7a)); 135.86 (*s*, C(1′)); 133.97 (*s*, C(4′)); 133.43 (*s*, C(5)); 132.36 (*s*, C(3′, C(5′)); 131.83 (*s*, C(2′), C(6′)); 131.20 (*s*, C(7)); 129.03 (*d*, C(3)); 128.81 (*s*, C(6)); 126.04 (*s*, C(4)); 43.13 (*t*, C(1)); 18.16 (*q*, *Me*–C(2′), *Me*–C(6′)); 16.71 (*q*, *Me*–C(4′) or *Me*–C(5) or

Me–C(6)); 16.63 (*q*, *Me*–C(7)); 16.53 (*q*, *Me*–C(3′), *Me*–C(5′)); 16.32 (*q*, *Me*–C(4)); 16.10 (*q*, *Me*–C(4′) or *Me*–C(5) or *Me*–(6)); 15.97 (*q*, *Me*–C(4′) or *Me*–C(5) or *Me*–C(6)). EI-MS: 318.1 (100, $M^{+\bullet}$, $C_{24}H_{30}^{+\bullet}$), 303.1 (80, $[M-Me]^+$), 288.1 (94, $[M-2\,Me]^+$), 147.0 (52, $[Me_5C_6]^{+\bullet}$). CI-MS: 319.3 (100, $[M+1]^{+\bullet}$), 305.3 (6, $[M+1-Me]^{+\bullet}$).

1.2. *Cross Experiment with* **1a** *and 4,6,8-Trimethyl-2*H*-cyclohepta[*b*]furan-2-one* (**1b**). A mixture of **1a** (1.26 g, 5.8 mmol) and **1b** (3.28 g, 17.4 mmol) in decaline (40 ml) was stirred under Ar at 180°. After 18 h, the mixture was worked up according to *Exper. 1.1.* Repetitive CC yielded **4ba** (0.218 g, 12%), **5ba** (0.026 g, 2.6%), colorless **6a** (0.045 g, 4.9%), and recovered **1a** (0.06 g, 5%) and **1b** (2.42 g, 74%).

Data of 4,6,8-Trimethyl-2-(2,3,4,5,6-pentamethylphenyl)azulene (**4ba**): Violet-blue crystals. M.p. 188.5–192.4° (hexane). UV/VIS (hexane): 560 (sh, 2.64), 537 (266), 372 (sh, 3.40), 355 (3.79), 340 (3.63), 314 (4.26), 292 (4.69), 242 (4.37), 199 (4.67); min. 415 (1.87), 345 (3.62), 332 (3.60), 261 (3.78), 232 (4.30). ^{1}H-NMR (600 MHz, C_6D_6): 7.34 (*s*, H–CH(1,3)); 6.85 (*s*, H–C(5,7)); 2.65 (*s*, Me–C(4,8)); 2.32 (*s*, Me–C(6)); 2.24 (*s*, Me–C(4′)); 2.21 (*s*, Me–C(3′,5′)); 2.20 (*s*, Me–C(2′,6′)). ^{13}C-NMR (150 MHz, C_6D_6): 150.62 (*s*, C(2)); 144.89 (*s*, C(6)); 144.65 (*s*, C(4,8)); 138.07 (*s*, C(1′)); 137.68 (*s*, C(3a,8a)); 133.86 (*s*, C(4′)); 132.40 (*s*, C(3′,5′)); 132.19 (*s*, C(2′,6′)); 127.89 (*d*, C(5,7)); 118.29 (*d*, C(1,3)); 28.77 (*q*, *Me*–C(6)); 25.28 (*q*, *Me*–C(4,8)); 19.58 (*q*, *Me*–C(2′,6′)); 17.18 (*q*, *Me*–C(4′)); 17.09 (*q*, *Me*–C(3′,5′)). EI-MS: 316.1 (96, $M^{+\bullet}$), 301.1 (72, $[M-Me]^+$), 286.1 (100, $[M-2\,Me]^+$), 271.0 (60, $[M-3\,Me]^+$). Anal. calc. for $C_{24}H_{28}$ (316.48): C 91.08, H 8.92; found: C 90.91, H 9.05.

1.3. *Cross Experiment with* **1a** *and Cyclohepta[*b*]furan-2-one* (**1c**). According to *Exper.1.2*, a mixture of **1a** (0.013 g, 0.062 mmol) and **1c** (0.009 g, 0.062 mmol) in decalin (0.5 ml) was stirred in a *Schlenk* vessel during 2.5 h at 230°. HPLC/UV and GC/MS (*Spherisorb CN*, 3 μm; 125 × 40 mm; hexane) of a raw reaction mixture, before chromatography, confirmed the presence of **4ca**, **4a**, **5ca**, **5a**, and **6a**; HPLC/UV: **4ca**/**4a**/**5ca**/**5a**/**6a** 17.4 : 5.8 : 6.2 : 1 : 6.6. Workup according to *Exper. 1.1* gave **4ca** (3.1 mg, 18.3%), **5ca** (0.1 mg, 1.2%), **1a** (0.0016 g, 12%), **1c** (4.4 mg, 49%), and **4a**/**5a**/**6a** (2.6 mg).

Data of 2-(2,3,4,5,6-Pentamethylphenyl)azulene (**4ca**): Blue crystals. M.p. 180.5–186.2° (hexane). UV/VIS (hexane): 672 (2.10), 613 (2.41), 569 (2.44), 545 (sh, 2.32), 365 (sh, 3.32), 347 (3.62), 330 (sh, 3.63), 317 (3.93), 302 (4.15), 282 (4.72), 275 (4.71), 232 (sh, 4.20), 200 (4.66); min. 439 (1.67), 363 (3.32), 340 (3.56), 315 (3.92), 300 (4.15), 278 (4.70), 251 (4.05). ^{1}H-NMR (600 MHz, $CDCl_3$): 8.31 (*d*, $^3J(4,5) = {}^3J(8,7) = 9.2$, H–C(4,8)); 7.57 (*t*, $^3J(6,5) = {}^3J(6,7) = 9.9$, H–C(4,8)); 7.22 (*s*, H–C(1,3)); 7.20 (*t*, $^3J(5,4) = {}^3J(5,6) = {}^3J(7,6) = {}^3J(7,8) = 9.8$, H–C(5,7)); 2.34 (*s*, Me–C(4′)); 2.29 (*s*, Me–C(3′,5′)); 1.97 (*s*, Me–C(2′,6′)). ^{13}C-NMR (150 MHz, $CDCl_3$): 153.72 (*s*, C(2)); 140.32 (*s*, C(3a,8a)); 136.36 (*s*, C(1′)); 136.10 (*d*, C(6)); 135.40 (*d*, C(4,8)); 134.22 (*s*, C(4′)); 132.28 (*s*, C(3′,5′)); 131.70 (*s*, C(2′,6′)); 123.09 (*d*, C(5,7)); 119.21 (*d*, C(1,3)); 18.69 (*q*, Me–C(2′,6′)); 16.80 (*q*, *Me*–C(4′)); 16.56 (*q*, *Me*–C(3′,5′)). EI-MS: 274.1 (97, $M^{+\bullet}$, $C_{21}H_{22}^{+\cdot\cdot}$), 259.1 (100, $[M-Me]^+$), 244.0 (92, $[M-2\,Me]^+$), 229.0 (90, $[M-3\,Me]^+$).

2. *Reaction of* **1a** *with 1-Ethynyl-2,3,4,5,6-pentamethylbenzene* (**9a**). 2.1. *1-Ethynyl-2,3,4,5,6-pentamethylbenzene* (**9a**). In analogy to [18]: Phosphorous trichloride (11.5 ml, 131 mmol) was mixed with (2,3,4,5,6-pentamethylphenyl)ethanone (6.0 g, 28.9 mmol; *Avocado* Comp.) in toluene (30 ml). Pentachlorophosphorane (12.6 g, 60 mmol) was added and the mixture heated at 55° for two weeks. Nonreacted PCl_5 and PCl_3 were removed *in vacuo*. The residue was washed with H_2O and dried. CC (silica gel, hexane/Et_2O 9 : 1) gave colorless crystals of *1-(1-chloroethenyl)-2,3,4,5,6-pentamethylbenzene* (3.45 g, 63%). Colorless crystals. M.p. 73.5–75.5° (hexane/Et_2O). ^{1}H-NMR (300 MHz, $CDCl_3$): 5.94 (br. *s*, 1 H, CH_2); 5.48 (br. *s*, 1 H, CH_2); 2.57 (*s*, 2 Me); 2.49 (*s*, Me–C(4)); 2.47 (*s*, Me–C(2,6)). ^{13}C-NMR (75 MHz, $CDCl_3$): 140.19 (*s*); 136.56 (*s*); 135.69 (*s*); 132.67 (*s*); 131.26 (*s*); 116.71 (*d*, CH_2); 17.46 (*q*, 2 Me); 16.90 (*q*, Me–C(4)); 16.49 (*q*, 2 Me). EI-MS: 207.9, 210.0 (100, 70, $M^{+\bullet}$, $C_{13}H_{17}Cl^{+\bullet}$), 193.1, 195.1 (44, 14 $[M-Me]^+$), 173.0 (98, $[M-Cl]^+$), 158.1 (81, $[M-Cl-Me]^+$).

The pure (chloroethenyl)benzene (2.42 g, 11.6 mmol) was dissolved in dry THF (20 ml) and added dropwise within 0.5 h to a stirred suspension of lithium diisopropylamide at −78°, prepared at −78° from 2.5M BuLi in hexane (12 ml, 30 mmol) and diisopropylamine (5 ml, 36 mmol) in THF (12 ml). The mixture was allowed to warm to r.t., and stirring was continued for 6 h. The reaction was quenched by the addition of cold H_2O (10 ml), the org. layer formed was washed with dil. HCl soln. (10 ml; conc. HCl soln./H_2O 1 : 10) and H_2O, and evaporated, and the crude product was purified by sublimation and recrystallized from hexane: pure **9a** (1.19 g, 60%). Colorless crystals. M.p. 90.2–92.7° (hexane). IR ($CHCl_3$): 3307*s* (H–C≡C); 2096*w* (C≡C). ^{1}H-NMR (300 MHz, $CDCl_3$): 3.47 (*s*, H–C≡C); 2.49 (*s*, 2 Me); 2.27 (*s*, Me–C(4)); 2.24 (*s*, Me–C(2′,6′)). ^{13}C-NMR (75 MHz, $CDCl_3$): 136.02 (*s*); 135.65 (*s*); 132.19 (*s*); 119.75 (*s*); 83.75 (*d*, HC≡C); 83.04 (*s*, HC≡*C*); 18.59 (*q*, 2 Me); 16.75 (*q*, *Me*–C(4)); 16.42 (*q*, 2 Me). EI-MS: 172.1 (100, $M^{+\bullet}$, $C_{13}H_{16}^{+\cdot\cdot}$), 157.1 (94, $[M-Me]^+$), 142.1 (88, $[M-2\,Me]^+$), 229.0 (90, $[M-3\,Me]^+$).

2.2. *Thermal Reaction of* **1a** *and* **9a**: *Formation of 4,5,6,7,8-Pentamethyl-9-(2,3,4,5,6-pentamethylphenyl)-6,8a-etheno-8a*H*-cyclohepta[*b*]furan-2*(6 H)*-one* (**11a**): A *Schlenk* vessel was charged with **1a** (0.030 g, 0.139 mmol) and **9a** (0.096 g, 0.555 mmol) in decalin (10 ml). The vessel was flushed with Ar, closed, and heated at 190° during 15 h. The solvent was then evaporated. The residual red solid was subjected to sublimation (120°/0.04 mbar) to remove nonreacted **9a** (0.048 g, 50%). CC (hexane/E_2O 9 :1) of residue gave, according to ^{1}H-NMR, pure **11a** (0.048 g, 89%). Rose crystals. M.p. 139.2 – 143.4° (hexane/Et_2O 9 :1). UV (hexane): 369 (sh, 2.82), 309 (sh, 3.55), 266 (3.99), 240 (sh, 4.00), 201 (4.71); min. 249 (3.92). IR ($CHCl_3$): 1742v*s* (C=O). ^{1}H-NMR (600 MHz, $CDCl_3$): 5.69 (*s*, H–C(10)); 5.57 (*s*, H–C(3)); 2.20 (*s*, Me–C(4′)); 2.19 (*s*, Me–C(5′)); 2.13 (*s*, Me–C(3′)); 2.09 (br. s, Me–C(5)); 2.05 (*s*, Me–C(6′)); 1.88 (*d*-like, $^5J(4,5) = 1{,}2$, Me–C(4)); 1.87 (*s*, Me–C(2′)); 1.84 (*d*-like, $^5J(7,8) = 1.0$, Me–C(7)); 1.77 (*d*-like, $^5J(8,7) = 1.2$, Me–C(8)); 1.56 (*s*, ME–C(6)). ^{13}C-NMR (150 MHz, $CDCl_3$): 173.9 (*s*, C(2)); 162.62 (*s*, C(3a)); 149.45 (*s*, C(5)); 144.02 (*s*, C(9)); 137.29 (*s*, C(7)); 135.65 (*d*, C(10)); 134.23 (*s*, C(4′)); 133.35 (*s*, C(6′)); 132.13 (*s*, C(1′)); 132.03 (*s*, C(5′)); 131.98 (*s*, C(3′)); 131.62 (*s*, C(8)); 131.52 (*s*, C(2′)); 119.90 (*s*, C(4)); 108.09 (*d*, C(3)); 90.96 (*s*, C(8a)); 49.46 (*s*, C(6)); 23.25 (*q*, *Me*–C(6)); 18.71 (*q*, *Me*–C(6′)); 18.10 (*q*, *Me*–C(5)); 17.66 (*q*, *Me*–C(2′)); 16.70 (*q*, *Me*–C(4)); 16.66 (*q*, *Me*–C(4′)); 16.55 (*q*, *Me*–C(3′)); 16.41 (*q*, *Me*–C(5′)); 14.62 (*q*, *Me*–C(7)); 11.37 (*q*, *Me*–C(8)). EI-MS: 388.2 (100, $M^{+\bullet}$), 373.2 (83, $[M - Me]^+$), 202 (75, $C_{13}H_{14}O_2^+$). Anal. calc. for $C_{27}H_{32}O_2 \cdot 0.33\ H_2O$ (394.54): C 82.19, H 8.35; found: C 82.08, H 8.19.

3. *Thermal Reaction of the New Azulenes with ADM*. 3.1. *Formation of Dimethyl 6,7,8,9,10-Pentamethylheptalene-4,5-dicarboxylate* (**20**). Azulene **5a** (0.050 g, 0.252 mmol) was dissolved in toluene (2 ml) under Ar in a flame-dired *Schlenk* vessel, and ADM (0.093 ml, 0.757 mmol) was added. The vessel was flushed again with Ar and then closed. The dark blue soln. was heated at 120 – 130°. It turned immediately to a deep orange color. After 25 min of stirring at 120 – 130°, the solvent and unreacted ADM were evaporated at 50°. The residual orange solid was subjected to flash CC (silica gel, hexane/Et_2O 1 :1). From the main yellow fraction, pure **20** (0.014 g, 16%) was obtained. For NMR and UV/VIS characterization of its DBS isomer **20′**, a $CDCl_3$ soln. of **20** was irradiated in an NMR tube with a high-pressure Hg lamp. After 1 h of irradiation, a photostationary mixture **20**/**20′** 54 :46 was obtained.

Data of **20**: Orange crystals. M.p. 102.3 – 105.9° (hexane). UV/VIS (hexane): tailing up to > 400, 289 (sh, 3.98), 254 (4.21), 234 (sh, 4.26), 219 (4.37); min. 247 (4.20). Ir ($CHCl_3$): 1716v*s* (C=O), 1266*s* (C–O). ^{1}H-NMR (600 MHz, $CDCl_3$): 7.51 (*d*, $^3J(3,2) = 6.2$, H–C(3)); 6.26 (*dd*, $^3J(2,3) = 6.3$, $^3J(2,1) = 10.2$, H–C(2)); 6.20 (*d*, $^3J(1,2) = 10.2$, H–C(1)); 3.73 (*s*, MeOCO–C(4)); 3.67 (*s*, MeOCO–C(5)); 1.96 (*s*, Me–C(8)); 1.85 (*s*, Me–C(9)); 1.80 (*s*, Me–C(6), Me–C(7)); 1.76 (*s*, Me–C(10)). ^{13}C-NMR (150 MHz, $CDCl_3$): 168.14 (*s*, O=*C*–C(5)); 167.53 (*s*, O=*C*–C(4)); 150.32 (*s*, C(5a)); 139.18 (*s*, C(8)); 138.56 (*d*, C(3)); 134.58 (*s*, C(7)); 133.45 (*s*, C(10)); 133.39 (*s*, C(4)); 133.21 (*d*, C(1)); 132.16 (*s*, C(9)); 128.61 (*s*, C(6)); 128.29 (*s*, C(10a)); 126.85 (*d*, C(2)); 122.54 (*s*, C(5)); 52.05 (*q*, *Me*OCO–C(4)); 51.86 (*q*, *Me*OCO–C(5)); 20.17 (*q*, *Me*–C(6)); 18.75 (*q*, *Me*–C(8)); 17.59 (*q*, *Me*–(7)); 17.28 (*q*, *Me*–C(9)); 15.66 (*q*, *Me*–C(10)). EI-MS: 340.1 (61, $M^{+\bullet}$, $C_{21}H_{24}O_4^{+\bullet}$), 325.0 (30, $[M - Me]^+$), 308.0 (18, $[M - MeOH]^+$), 293.0 (57, $[M - MeOH - Me]^+$), 286.0 (24, $[M - MeC{\equiv}CMe]^+$), 281.1 (100, $[M - COOMe]^+$), 266.0 (83, $[M - COOMe - Me]^+$), 254.0 (59, $[M - MeC{\equiv}CMe - MeOH]^+$), 249.0 (83, $[M - COOMe - MeOH]^+$), 239.0 (78, $[M - MeOH - Me - MeC{\equiv}CMe]^+$).

Data of Dimethyl 6,7,8,9,10-Pentamethylheptalene-1,2-dicarboxylate (**20′**): UV/VIS (hexane; taken from the photo-stationary mixture with the HPLC/UV detector; rel. intensities with respect to the strongest band intensity = 100%): 367 (4), 271 (69), 227 (sh, 83), 208 (100); min. 359 (3), 252 (63). ^{1}H-NMR (600 MHz, $CDCl_3$; taken from the photo-stationary mixture): 6.69 (*dd*, $^3J(4,5) = 6.0$, $^3J(4,3) = 11.5$, H–C(4)); 6.52 (*d*, $^3J(3,4) = 11.5$, H–C(3)); 5.79 (*d*, $^3J(5,4) = 6.0$, H–C(5)); 3.83 (*s*, MeOCO–C(2)); 3.73 (*s*, MeOCO–C(1)); 1.95 (*s*, Me–C(6)); 1.92 (*s*, Me–C(8)); 1.86 (*s*, Me–C(7)); 1.83 (*s*, Me–C(9)); 1.70 (*s*, Me–C(10)). ^{13}C-NMR (150 MHz, $CDCl_3$; taken from the photo-stationary mixture): 168.60 (*s*, O=*C*–C(2)); 167.21 (*s*, O=*C*–C(1)); 147.09 (*s*, C(5a)); 138.66 (*s*, C(8)); 137.02 (*s*, C(2)); 135.22 (*d*, C(4)); 134.76 (*s*, C(7)); 134.37 (*s*, C(10)); 132.70 (*s*, C(9)); 132.05 (*s*, C(6)); 126.86 (*s*, C(10a)); 125.30 (*d*, C(3)); 124.90 (*s*, C(1)); 121.43 (*d*, C(5)); 52.56 (*q*, MeOCO–C(2)); 52.35 (*q*, *Me*OCO–C(1)); 20.95 (*q*, *Me*–C(6)); 19.08 (*q*, *Me*–C(8)); 18.08 (*q*, *Me*–C(7)); 17.64 (*q*, *Me*–C(9)); 15.26 (*q*, *Me*–C(10)).

3.2. *Formation of Dimethyl 6,8,10-Trimethyl-2-(2,3,4,5,6-pentamethylphenyl)heptalene-4,5-dicarboxylate* (**22**). Azulene **4ba** (0.070 g, 0.221 mmol) was dissolved in toluene (1.5 ml) under Ar in a flame-dried *Schlenk* vessel, and ADM (0.082 ml, 0.664 mmol) was added. The vessel was flushed again with Ar and then closed. The dark blue soln. was heated at 120 – 130°. After 20 h, a second portion of ADM (0.082 ml, 0.664 mmol) was added and heating continued for additional 10 h. The solvent and unreacted ADM were evaporated at 50°. The residual orange solid was subjected to CC (silica gel, hexane/Et_2O 1 :1). The yellow main fraction (0.068 g) gave,

after crystallization from hexane at −18°, **22** (0.035 g, 34%). According to ^{1}H-NMR ($CDCl_3$), **22** reacted rapidly at 20° to a thermal equilibrium mixture of 87% of **22** and 13% of its DBS isomer **22′**. From a second blue fraction of CC, the known *dimethyl 4,6,8-trimethylazulene-1,2-dicarboxylate* (**23**, 6.0 mg, 9%) was isolated.

The thermal reaction **4ba** (0.070 g, 0.221 mmol) and ADM (0.082 ml, 0.664 mmol) in tetralin (=1,2,3,4-tetrahydronaphthalene; 1,5 ml) at 205°/6 h gave **22** (0.036 g, 36%) and **23** (4.0 mg, 6%), whereby 30% of non-reacted **4ba** (0.021 g) were recovered.

Data of **22**: Orange crystals. M.p. 178.5–181.7° (hexane). UV/VIS (hexane soln. of the thermal equilibrium mixture): tailing from >400, 334 (sh, 3.57), 267 (4.27), 222 (sh, 4.51); min. 251 (4.24). UV/VIS (hexane; taken from the thermal equilibrium mixture by HPLC/UV; see above): tailing from >400. 325 (sh, 12), 262 (41), 212 (100); min. 250 (38). IR ($CHCl_3$): 1716v*s* (C=O), 1270v*s* (C–O), 1252v*s* (C–O). ^{1}H-NMR (600 MHz, $CDCl_3$; taken from the thermal equilibrium mixture)[5]): 7.44 (*s*, H–C(3)); 6.20 (*s*, H–C(9)); 6.00 (*s*, H–C(7)); 5.79 (*s*, H–C(1)); 3.73 (*s*, MeOCO–C(5)); 3.70 (*s*, MeOCO–C(4)); 2.31 (*s*, Me–C(2′)); 2.28 (*s*, Me–C(4′)); 2.27 (*s*, Me–C(3′)); 2.22 (*s*, Me–C(5′)); 2.08 (*s*, Me–C(6′)); 2.06 (br. *s*, Me–C(8)); 2.04 (*d*, $^4J(6,7)=1.2$, Me–C(6)); 1.83 (*s*, Me–C(10)). ^{13}C-NMR (75 MHz, $CDCl_3$; taken from the thermal equilibrium mixture): 167.93 (*s*, O=*C*–C(5)); 167.26 (*s*, O=*C*–C(4)); 148.18 (*s*, C(5a)); 143.40 (*s*, C(2)); 142.83 (*d*, C(3)); 139.93 (*s*, C(8)); 136.88 (*s*, C(1′)); 134.42 (*s*, C(4′)); 133.06 (*d*, C(1); C(2′)); 130.13 (superimposed *d* and *s*, C(9), C(6)); 129.32 (*d*, C(7)); 123.08 (*s*, C(5)); 122.34 (*s*, C(10a)); signal of C(4) (*s*) not recognizable; 52.00 (*q*, *Me*OCO–C(4)); 51.94 (*q*, *Me*OCO–C(5)); 24.95 (*q*, *Me*–C(8)); 23.21 (*q*, *Me*–C(6)); 18.14 (*q*, *Me*–C(2′)); 17.90 (*q*, *Me*–C(10)); 17.16 (*q*, *Me*–C(6′)); 16.75 (*q*, *Me*–C(4′)); 16.58 (*q*,*Me*–C(3′)); 16.37 (*q*, *Me*–C(5′)). EI-MS: 458.1 (100, $M^{+\bullet}$, $C_{30}H_{34}O_4^{+\bullet}$), 399.1 (36, $[M-COOMe]^+$).

The structure of **22** was confirmed by an X-ray crystal-structure analysis (*cf.* below).

Data of Dimethyl 6,8,10-Trimethyl-4-(2,3,4,5,6-pentamethylphenyl)-heptalene-1,2-dicarboxylate (**22′**): UV/VIS (hexane; taken from the thermal equilibrium mixture by HPLC/UV; see above): tailing from >400, 317 (sh, 15), 272 (48), 218 (sh, 80), 204 (100); min. 252 (38). ^{1}H-NMR (600 MHz, $CDCl_3$; taken from the thermal equilibrium mixture)[5]): 6.28 (*d*, $^4J(3,5)=0.8$, H–C(3)); 6.12 (*s*, H–C(9)); 5.89 (*s*, H–C(7)); 5.61 (*d*, $^4J(5,3)=0.8$, H–C(5)); 3.83 (*s*, MeOCO–C(2)); 3.72 (*s*, MeOCO–C(1)); 2.23 (*s*, Me–C(4′)); 2.21 (*s*, Me–C(3′)); 2.16 (*s*, Me–C(2′), Me–C(5′)); 2.10 (*s*, Me–C(6)); 1.94 (*s*, Me–C(8)); 1.90 (*s*, Me–C(6′)); 1.74 (*s*, Me–C(10)).

3.3. *Formation of Dimethyl 6,7,8,9,10-Pentamethyl-2-(2,3,4,5,6-pentamethylphenyl)heptalene-4,5-dicarboxylate* (**24**). As described in *Exper. 3.1*, **4a** (0.070 g, 0.203 mmol) and ADM (0.125 ml, 1.02 mmol) in toluene (2.0 ml) gave, after 50 min of heating at 120°, followed by CC and crystallization from hexane, **24** (0.038 g, 39%). The ^{1}H-NMR (500 MHz; $CDCl_3$) of the crude **24** indicated the presence of a second product **27** (total amount *ca.* 3%), which was also found in crystalline **24** as yellow crystals that could be separated mechanically from the crystal mixture. For NMR and UV/VIS characterization of the DBS isomer **24′** of **24**, a dioxane soln. (1 ml) of **24** (0.020 g) was irradiated in a UV cuvette with a high-pressure Hg lamp. After 4 h of irradiation, a photostationary mixture **24**/**24′** 63:37 was obtained. The DBS isomer **24′** (5.0 mg, 25%) was separated by prep. TLC (hexane/*t*-BuOMe 9:1).

Data of **24**: Orange crystals. M.p. 181.2–183.5° (hexane). UV/VIS (hexane): tailing from >400, 291 (sh, 4.07), 257 (4.33), 226 (4.47); min. 245 (4.31). IR ($CHCl_3$): 1714v*s* (C=O), 1268v*s* (C–O), 1252v*s* (C–O). ^{1}H-NMR (500 MHz, $CDCl_3$)[5]): 7.39 (*s*, H–C(3)); 5.92 (*s*, H–C(1)); 3.70 (*s*, MeOCO–C(4), MeOCO–((5)); 2.31 (*s*, Me–C(2′)); 2.28 (*s*, Me–C(3′), Me–C(4′)); 2.21 (*s*, Me–C(5′)); 2.03 (*s*, Me–C(6′)); 1.98 (*s*, Me–C(8)); 1.88 (*s*, Me–C(9)); 1.87 (*s*, Me–C(6)); 1.83 (*s*, Me–C(7)); 1.80 (*s*, Me–C(10)). ^{13}C-NMR (125 MHz, $CDCl_3$): 168.09 (*s*, O=*C*–C(5)); 167.43 (*s*, O=*C*–C(4)); 151.23 (*s*, C(5a)); 141.25 (*d*, C(3)); 141.16 (*s*, C(2) or C(4)); 138.75 (*s*, C(8)); 137.27 (*s*, C(1′)); 134.31 (*s*, C(4′)); 134.18 (*s*, C(7)); 133.22 (*s*, C(10)); 132.69 (*s*, C(2′) or C(3′)); 132.50 (*s*, C(2) or C(4)); 132.48 (*s*, C(5′)); 132.45 (*s*, C(6′)); 132.27 (*s*, C(9)); 131.68 (*d*, C(1)); 130.53 (*s*, C(2′) or C(3′)); 128.36 (*s*, C(6)); 127.89 (*s*, C(10a)); 121.95 (*s*, C(5)); 51.98, 51.86 (*q*, *Me*OCO–C(4), *Me*OCO–C(5)); 20.17 (*q*, *Me*–C(6)); 18.84 (*q*, *Me*–C(8)); 18.18 (*q*, *Me*–C(2′)); 17.62 (*q*, *Me*–C(7)); 17.34 (*q*, *Me*–C(9)); 17.24 (*q*, *Me*–C(6′)); 16.76, 16.64 (*q*, *Me*–C(3′), *Me*–C(4′)); 16.39 (*q*, *Me*–C(5′)); 15.86 (*q*, *Me*–C(10)). EI-MS: 486.3 (54, $M^{+\bullet}$), 432.2 (35, $[M-MeC{\equiv}CMe]^+$), 427.2 (100, $[M-COOMe]^+$), 395.2 (25, $[M-COOMe-MeOH]^+$), 385.2 (14, $[M-MeOH-Me-MeC{\equiv}CMe]^+$), 299.1 (22, $[M-Me_5C_6-Me]^+$). Anal. calc. for $C_{32}H_{38}O_4$ (486.64): C 78.98, H 7.87; found: C 79.04, H 7.78.

The structure of **24** was confirmed by an X-ray crystal-structure analysis (*cf.* below).

---

[5]) For the 2-(2,3,4,5,6-pentamethylphenyl)heptalene derivatives, the (*P*)-chirality was chosen arbitrarily for the assignment of the ^{1}H- and ^{13}C-signals of the diastereoisomeric C-atoms and Me groups, whereby the (pro-*P*) atoms or groups were given priority.

Data of Dimethyl 6,7,8,9,10-Pentamethyl-4-(2,3,4,5,6-pentamethylphenyl)heptalene-1,2-dicarboxylate (**24′**): Orange crystals. M.p. 183.0–187.5° (hexane). UV/VIS (hexane): tailing up to >400, 357 (sh, 3.14), 270 (sh, 4.17), 219 (sh, 4.51), 199 (4.80); min. not present down to 200. IR ($CHCl_3$): 1721v*s* (C=O), 1268*s* (C–O), 1236*s* (C–O). ^{1}H-NMR (600 MHz, $CDCl_3$)[5]): 6.31 (*d*, $^4J(3,5) = 0.5$, H–C(3)); 5.45 (*s*, $^4J(5,3) = 0.5$, H–C(5)); 3.83 (*s*, MeOCO–C(2)); 3.77 (*s*, MeOCO–C(1)); 2.23 (*s*, Me–C(4′)); 2.22 (*s*, Me–C(3′)); 2.18 (*s*, Me–C(2′)); 2.16 (MeOCO–C(1)); 2.23 (*s*, Me–C(4′)); 2.22 (*s*, Me–C(3′)); 2.18 (*s*, Me–C(2′)); 2.16 (*s*, Me–C(5′)); 2.96 (*s*, Me–C(6)); 1.86 (*s*, Me–C(8)); 1.82 (*s*, Me–C(7)); 1.81 (*s*, Me–C(9)), 1.78 (*s*, Me–C(6′)); 1.77 (*s*, Me–C(10)). ^{13}C-NMR (150 MHz, $CDCl_3$): 168.57 (*s*, O=*C*–C(2)); 167.04 (*s*, O=*C*–C(1)); 150.03 (*s*, C(4)); 147.81 (*s*, C(5a)); 139.80 (*s*, C(1′)); 138.25 (*s*, C(8)); 137.06 (*s*, C(2)); 134.22 (*s*, C(10)); 133.99 (*s*, C(4′)); 133.95 (*s*, C(7)); 132.41 (*s*, C(9), C(3′)); 132.28 (*s*, C(5′)); 132.05 (*s*, C(6)); 131.46 (*s*, C(6′)); 129.48 (*s*, C(2′)); 127.84 (*s*, C(10a)); 125.51 (*s*, C(1)); 124.89 (*d*, C(3)); 123.78 (*s*, C(5)); 52.44 (*q*, *Me*OCO–C(2)); 52.29 (*q*, *Me*OCO–C(2)); 20.48 (*q*, *Me*–C(6)); 18.77 (*q*, *Me*–C(8)); 18.06 (*q*, *Me*–C(2′)); 17.69 (*q*, *Me*–C(7)); 17.26 (*q*, *Me*–C(9)); 16.69 (*q*, *Me*–C(4′)); 16.65 (*q*, *Me*–C(6′)); 16.50 (*q*, *Me*–C(3′)); 16.36 (*q*, *Me*–C(5′)); 15.37 (*q*, *Me*–C(10)).

Data of Dimethyl 5,6,7,8-Tetramethyl-2-(2,3,4,5,6-pentamethylphenyl)acenaphthalene-3,4-dicarboxylate (**27**): Yellow crystals.M.p. 241.3–243.3° (hexane). UV/VIS (hexane): 359 (sh, 3.79), 338 (3.98), 327 (sh, 3.87), 255 (4.55), 223 (sh, 4.58), 202 (4.85); min. 298 (3.66), 241 (4.46). IR ($CHCl_3$): 1726v*s* (C=O), 1250*s* (C–O). ^{1}H-NMR (600 MHz, $CDCl_3$): 6.82 (*s*, H–C(1)); 3.62 (*s*, MeOCO–C(4)); 2.91 (*s*, MeOCO–C(3)); 2.70 (*s*, Me–C(5)); 2.31 (*s*, Me–C(6)); 2.25 (*s*, Me–C(2′), Me–C(6′)); 2.18 (*s*, Me–C(8)); 2.15 (*s*, Me–C(4′)); 2.14 (*s*, Me–C(3′), Me–C(5′)); 2.00 (*s*, Me–C(7)). ^{13}C-NMR (150 MHz, $CDCl_3$): 170.26 (*s*, O=*C*–C(4)); 168.66 (*s*, O=*C*–C(4)); 143.00 (*s*, C(2)); 137.81 (*s*, C(7)); 136.95 (*s*, C(8a)); 136.85 (*s*, C(8b)); 136.52 (*s*, C(8)); 136.48 (*s*, C(5) or C(4)); 135.09 (*s*, C(6)); 134.79 (*s*, C(1′)); 133.81 (*s*, C(4′)); 133.29 (*s*, C(2′), C(6′)); 133.09 (*s*, C(5) or C(4)); 132.34 (*s*, C(3′), C(5′)); 129.63 (*s*, C(5a)); 129.16 (*s*, C(2a)); 128.68 (*s*, C(3)); 128.36 (*d*, C(1)); 52.30 (*q*, *Me*OCO–C(4)); 51.51 (*q*, *Me*OCO–C(3)); 22.41 (*q*, *Me*–C(5)); 20.63 (*q*, *Me*–C(6)); 19.04 (*q*, *Me*–C(2′), *Me*–C(6′)); 17.92 (*q*, *Me*–C(8)); 17.04 (*q*, *Me*–C(7), *Me*–C(4′)); 16.88 (*q*, *Me*–C(3′), *Me*–C(5′)). EI-MS: 470.2 (100, $M^{+\bullet}$, $C_{31}H_{34}O_4^{+\bullet}$), 438.1 (25, $[M - MeO]^+$), 423.0 (84, $[M - Me - MeO]^+$), 379.1 (88, $[M - COOMe - MeOH]^+$).

The structure of **27** was confirmed by X-ray crystal-structure analysis (*cf.* below).

4. *Thermal Equilibration Experiments of the New Heptalenes.* 4.1. *Thermal Equilibration of* **20** *and* **20′**. A soln. of **20** (*ca.* 2 mg) in dioxane (0.2 ml) was heated 1 h at 100°. After heating, the probe was immediately subjected to HPLC (*Spherisorb CN*; hexane/^{i}PrOH 99.5 : 0.5; flow rate 1 ml/min): t_R 2.7 (**20′**) and 4.7 min (**20**); UV detection at the isosbestic point of the isomers (230 nm).

The photochemically prepared mixture **20**/**20′** 54 : 46 (*ca.* 1 mg) was dissolved in toluene (0.1 ml) and heated during 1.5 h at 100°. HPLC Analyses (time [min], **20**/**20′** [%]): 0, 54 : 46; 30, 87 : 13; 60, 89 : 11; 90, 90 : 10; no further changes in composition. $\tau_{1/2}(100°) \approx 22$ min.

4.2. *Thermal Equilibration of* **22** *and* **22′**. Heptalene **22** (*ca.* 5 mg) was dissolved in (D_8)toluene (0.6 ml). Equilibration occurred already at r.t. ^{1}H-NMR Analyses at 100°: equilibrium ratio **22**/**22′** of 74 : 26.

4.3. *Thermal Equilibration of* **24** *and* **24′**. A soln. of **24** (*ca.* 2 mg) in dioxane (0.2 ml) was heated 2 h at 100°. After heating, the probe was immediately subjected to HPLC (*Spherisorb CN*; hexane/^{i}PrOH 99.5 : 0.5; flow rate 1 ml/min): t_R 2.5 (**24′**) and 4.4 min (**24**). UV Detection at the isosbestic point of the isomers (286 nm) gave an equilibrium ratio **24**/**24′** of 84 : 16. The photochemically prepared **24′** (*ca.* 1 mg) was dissolved in toluene (0.1 ml) and heated at 100°. At regular time intervals, samples were taken and immediately subjected to HPLC analysis. Results (time [min], **24**/**24′** [%]): 30, 44 : 56; 60, 65 : 35; 90, 76 : 24; 150, 83 : 17; 210, 84 : 16; no further changes in composition. $\tau_{1/2}$ (100°) *ca.* 45 min.

5. *X-Ray Crystal-Structure Determination of* **22**, **24**, *and* **27**. 5.1. *Heptalene* **22** *and Acenaphthylene* **27**[6]). All measurements were made on a *Rigaku AFC5R* diffractometer with graphite-monochromated MoK_α radiation (*cf. Table 6*) and a 12 kW rotating anode generator. The structures of **22** ($C_{30}H_{34}O_4$) and **27** ($C_{31}H_{34}O_4$) were solved and refined successfully with no unusual features. The three fused rings of **27** form a planar system, and the plane of the pentamethylphenyl ring lies almost perpendicular to this plane with the interplanar angle being 83.90(9)°. Similarly, the pentamethylphenyl ring of **22** is almost perpendicularly oriented with respect to the π-plane of the C(1)=C(2) bond (*Tables 4* and *5*).

---

[6]) Crystallographic date (excluding structure factors) for the structures reported here have been deposited with the *Cambridge Crystallographic Data Center* as supplementary publication nos. CCDC-161722 and 161723 for **22** and **27**, respectively. Copies of the data can be obtained, free of charge, on application to the CCDC, 12 Union Road, Cambridge CB2 1EZ, UK (fax: +44-(0)1223-336033; e-mail: deposit@ccdc.cam.ac.uk).

Table 6. *Crystallographic Data of Heptalene-4,5-dicarboxylates* **22** *and* **24** *and Acenaphthylene-3,4-dicarboxylate* **27**

	22	**27**	**24**
Crystallized from	hexane	hexane/Et_2O	hexane
Empirical formula	$C_{30}H_{34}O_4$	$C_{31}H_{34}O_4$	$C_{32}H_{38}O_4$
M_r	458.59	470.61	486.62
Crystal color, habit	yellow, prism	yellow, prism	yellow, prism
Crystal dimensions [mm]	$0.23 \times 0.38 \times 0.45$	$0.38 \times 0.43 \times 0.45$	$0.08 \times 0.14 \times 0.52$
Temperature [K]	173(1)	173(1)	183(1)
Crystal system	monoclinic	triclinic	monoclinic
Space group	$P2_1/n$ (#14)	$P\bar{1}$ (#2)	$P2_1/n$ (#14)
Z	4	2	4
Reflections for cell determination	25	25	8000
2θRange for cell determination [°]	25 – 38	38 – 40	5 – 56
Unit-cell parameters			
a [Å]	13.969(4)	8.905(3)	9.007(6)
b [Å]	8.744(3)	16.739(7)	16.4382(15)
c [Å]	20.803(2)	8.908(3)	17.4171(12)
α [°]	90	97.91(4)	90
β [°]	95.57(1)	106.61(3)	99.909(8)
γ [°]	90	86.26(4)	90
V [Å^3]	2529(1)	1259.8(8)	2735.9(4)
$F(000)$	984	504	1048
D_x [g cm^{-3}]	1.204	1.241	1.181
$\mu(\mathrm{Mo}K_\alpha)$ [mm^{-1}]	0.0784	0.0805	0.0760
Scan type	$\omega/2\theta$	$\omega/2\theta$	φ-oscill. scan
$2\theta_{(\max)}$ [°]	55	55	56
Total reflections measured	6439	6183	26021
Symmetry-independent reflections	5806	5810	6122
R_{int}	0.049	0.024	0.136
Reflections used ($I > 2\sigma(I)$)	3561	4124	2442
Parameters refined	308	317	338
Reflection/parameter ratio	11.6	13.0	7.2
Final R	0.0577	0.0523	0.1895
wR	0.0541	0.0496	0.4967
Weights: p in $w = [\sigma^2(F_o) + (pF_o)^2]^{-1}$	0.005	0.005	0.1000
Goodness-of-fit	2.126	2.843	2.188
Secondary extinction coefficient	$2.2(4) \cdot 10^{-7}$	$6(1) \cdot 10^{-7}$	0.046(8)
Final Δ_{max}/σ	0.0002	0.0002	0.007
$\Delta\rho$ (max; min) [e Å^{-3}]	0.28; −0.28	0.28; −0.24	0.74; −0.64
$\sigma(d(\mathrm{C-C}))$ [Å]	0.003 – 0.004	0.003	0.013 – 0.015

5.2. *Heptalene* **24**[7]). Intensity data were collected with an imaging plate detector system (*Stoe IPDS*) [19] with graphite-monochromated Mo$K\alpha$ radiation (*cf. Table 6*). A total of 167 images were exposed at a constant time of 5 min/image. Direct methods with SHELXS-97 [20] were used to solve the structure. All non-H-atoms were refined anisotropically. H-Atom positions were calculated after each refinement cycle. The bad R values for **24** are due to a crystal of minor quality with many twinned domains with different orientations. Crystals of better quality could not be obtained by further crystallization experiments. Despite this fact, the twisted structure of **24** could be unambiguously determined (*cf. Fig. 8* and *Tables 4* and *5*).

---

[7]) Further information on crystallographic data of the structure of **24** are available from Dr. *H. W. Schmalle*, Anorganisch-chemisches Institut der Universität, CH-8057 Zürich, Winterthurerstrasse 190.

REFERENCES

[1] M. Nagel, H.-J. Hansen, *Helv. Chim. Acta* **2000**, *83*, 1022.
[2] W. S. Trahanovsky, S. L. Emeis, A. S. Lee, *J. Org. Chem.* **1976**, *41*, 4044.
[3] V. Lellek, M. Nagel, H.-J. Hansen, *Helv. Chim. Acta*, in preparation.
[4] M. Nagel, Diploma Thesis, University of Zürich, 1997.
[5] Y. Saseda, *Bull. Chem. Soc. Jpn.* **1959**, *32*, 165.
[6] A. Linden, M. Meyer, P. Mohler, A. J. Rippert, H.-J. Hansen, *Helv. Chim. Acta* **1999**, *82*, 2274.
[7] G. Melone, Ph. D. Thesis, University of Zürich, 1999.
[8] J. A. Berson, *Acc. Chem. Res.* **1978**, *11*, 446.
[9] W. Bernhard, H.-R. Zumbrunnen, H.-J. Hansen, *Chimia* **1979**, *33*, 324.
[10] Y. Chen, R. W. Kunz, P. Uebelhart, R. H. Weber, *Helv. Chim. Acta* **1992**, *75*, 2447.
[11] K. Hafner, G. L. Knaup, H. J. Lindner, *Bull. Chem. Soc. Jpn.* **1988**, *61*, 155.
[12] A. A. S. Briquet, P. Uebelhart, H.-J. Hansen, *Helv. Chim. Acta* **1996**, *79*, 2282.
[13] W. Bernhard, P. Brügger, J. J. Daly, P. Schönholzer, R. H. Weber, H.-J. Hansen, *Helv. Chim. Acta* **1985**, *68*, 415.
[14] K. Hafner, G. L. Knaup, H. J. Lindner, H.-C. Flöter, *Angew. Chem.* **1985**, *97*, 209; *Angew. Chem., Int. Ed.* **1985**, *24*, 212.
[15] L. A. Paquette, *Pure Appl. Chem.* **1982**, *54*, 987; L. A. Paquette, T.-Z. J. Luo, Ch. E. Cottrell, A. E. Clough, L. B. Anderson, *J. Am. Chem. Soc.* **1990**, *112*, 239; L. A. Paquette, M. P. Trova, J. Luo, A. E. Clough, L. B. Anderson, *J. Am. Chem. Soc.* **1990**, *112*, 228.
[16] D. Laikov, H.-J. Hansen, unpublished results.
[17] G. M. Brooke, R. Matthews, S. Raymond, M. E. Harman, M. B. Hursthouse, *J. Fluorine Chem.* **1991**, *53*, 339.
[18] K. L. Evans, P. Prince, E. T. Huang, K. R. Boss, R. D. Gandour, *Tetrahedron Lett.* **1990**, *31*, 6753.
[19] Stoe & Cie., Version 2.92, Darmstadt, Germany.
[20] G. M. Sheldrick, *Acta Crystallogr. Sect. A* **1990**, *46*, 467; G. M. Sheldrick, 'Program for the Refinement of Crystal Structures', University of Göttingen, 1997.

Received April 7, 2001